

The Pennsylvania State University
The Graduate School
College of Earth and Mineral Sciences

**MICROWAVE-INDUCED PYROLYSIS OF CORN STOVER:
THE INFLUENCE OF POTASSIUM ON THE GAS FRACTION**

A Thesis in
Energy and Geo-Environmental Engineering

by
Bradley J. Hartwell

© 2010 Bradley J. Hartwell

Submitted in Partial Fulfillment
of the Requirements
for the Degree of

Master of Science

May 2010

The thesis of Bradley J. Hartwell was reviewed and approved* by the following:

Sarma V. Pisupati
Associate Professor of Energy and Mineral Engineering
Thesis Advisor

Dinesh K. Agrawal
Professor of The Materials, and Engineering Science & Mechanics
Director of Microwave Processing and Engineering Center

Caroline E. Burgess Clifford
Senior Research Associate at The EMS Energy Institute

Yaw D. Yeboah
Professor of Energy and Mineral Engineering
Head of the Department of Energy and Mineral Engineering

*Signatures are on file in the Graduate School

ABSTRACT

At the turn of the twenty-first century, climate change became a hot topic in the mainstream media, and as a result, a worldwide concern arose about the possibility of human activity causing recent global temperatures to increase. This concern, coupled with fossil fuel resources becoming increasingly scarce, has caused a push for alternative fuel research.

This work focuses on converting a renewable feedstock, corn stover, to produce a useful gaseous fuel. Corn stover is the portion of the corn plant that is left over after the corn has been harvested from the stalk. Corn stover was selected for this study due to its relatively low ash content, which in turn allows for removal of catalytic inorganic content that would interfere with the investigation of potassium's effects on conversion. The conversion process carried out in this study is pyrolysis, which is the thermal decomposition of organic matter in an oxygen-free environment. Different pyrolysis conditions determine whether bio-oil or biogas will be a major byproduct. This study's pyrolysis conditions are designed to maximize the biogas fraction, and more specifically, to produce a high quality syngas consisting of mainly H₂ and CO. Syngas can be efficiently burned in a small gas turbine to generate electricity, or utilized in a Fischer-Tropsch process to produce liquid fuel.

The objective of this study is to investigate the effects of potassium between conventional and microwave pyrolysis. This objective was met by carrying out laboratory scale pyrolysis experiments in both an electrical tube furnace, and a multimode microwave operating at 2.45 GHz. Three different corn stover samples were investigated: stripped (S), stripped with 0.7 percent potassium addition (K0.7), stripped with 3.5 percent potassium addition (K3.5). All feedstocks were brought to 700 °C in the conventional pyrolysis experiments. All feedstocks were brought to both 700 and 1000 °C in the microwave experiments in order to get a qualitative trend on the influence of microwave pyrolysis temperature. To get a quantitative understanding of potassium's response to microwave pyrolysis temperature, K3.5 was also brought to 800, 900 and 1100 °C in the microwave.

It was observed in both microwave and conventional pyrolysis that potassium's main effects on pyrolysis in order of descending influence are: inhibiting volatile release, promoting secondary cracking reactions of heavy hydrocarbons (oil) and promoting the decomposition reaction of

methane at 700 °C. Potassium did not however appear to promote the carbon/CO₂ heterogeneous reaction which would have rejuvenated catalyst sites for further methane decomposition, as proposed in a previous study [1]. Potassium was shown to significantly inhibit the release of oxygen containing volatiles during pyrolysis at temperatures 700 to 1100 °C, even with a loading of 0.7 percent. The result from this is a much larger char fraction when potassium was added. This inhibiting effect of potassium was found to be important at higher temperatures.

A consistent trend among all temperatures tested in this study was that in microwave pyrolysis, potassium addition decreased the oil fraction produced. This means that potassium promoted the secondary reactions that broke down the heavy hydrocarbons into non-condensable gases.

A potassium loading between 0.7 and 3.5 percent was found to promote the decomposition of methane reaction at 700 °C, but not at 1000 °C. The reason why the decomposition of methane was not observed at the higher temperature is because at higher temperatures, potassium's pyrolysis inhibiting affect is the dominant effect. As a result of this, there was no increase in H₂ at the expense of CH₄. Potassium's promoting of the decomposition of methane was 60 percent more pronounced in microwave pyrolysis compared to conventional pyrolysis at 700 °C. A likely reason for this difference is that in microwave heating, the potassium could have achieved temperatures much higher than the rest of the sample, because in microwave heating, microwave receptive materials reach much higher temperatures than adjacent materials. This anisothermal heating has been demonstrated to enhance reactions taking place within a sample [2]. Anisothermal conditions were the most likely reason for the microwave pyrolysis' increased methane decomposition reactions. Methane decomposition was promoted with a potassium loading between 0.7 and 3.5 percent.

The experiment that showed the best syngas production was for sample S brought to 1000 °C in the microwave. This experiment yielded 88 mL/g (ash free) of H₂ and 120 mL/g (ash free) of CO.

Table of Contents

List of Figures.....	vii
List of Tables	ix
Acknowledgements.....	x
 Chapter 1 INTRODUCTION.....	 1
1.1 Motivation.....	1
1.2 Literature Review.....	3
1.2.1 Effect of Feedstock	3
1.2.1.1 Biogas Optimization	3
1.2.1.2 Bio-oil Optimization.....	6
1.2.1.3 Effect of Inherent/Added Catalysts	7
1.2.1.4 Effect of Moisture Content	10
1.2.2 Effect of Reactor Type.....	11
1.2.2.1 Microwave Heating Theory.....	12
1.2.2.2 Biogas Optimization	14
1.2.2.3 Bio-oil Optimization.....	16
1.2.2.4 Char Optimization	17
1.2.3 Effect of Operating Conditions.....	18
1.2.3.1 Pyrolysis Temperature	18
1.2.3.2 Biogas Optimization	21
1.2.3.3 Bio-oil Optimization.....	21
1.2.3.4 Reactor Scaling.....	22
1.2.4 Effect of Microwaving Conditions	22
1.2.5 Conclusion and Recommendations.....	23
1.3 Problem Statement	23
1.4 Hypothesis.....	24
1.5 Research Objectives.....	24
 Chapter 2 METHODOLOGY	 26
2.1 Corn Stover Preparation.....	26
2.2 Experimental Setup.....	28
2.2.1 Pyrolysis Conditions	30
2.2.2 Pyrolysis Temperature	31
2.2.3 Calibrating Sample's Emissivity.....	32
2.2.4 Relating Microwave Power with Pyrolysis Temperature	32
2.2.5 Temperature Profiles.....	35
2.3 Methods for Product Analysis	36

2.3.1	Product Fractions	36
2.3.2	Char Methods.....	39
2.3.3	Bio-oil Methods	39
2.3.4	Bio-gas Methods.....	40
Chapter 3 EXPERIMENTAL RESULTS AND DISCUSSION.....		41
3.1	Product Fractions	41
3.1.1	Effect of Heating Method	42
3.1.2	Effect of Potassium Loading.....	44
3.1.3	Effect of Temperature	47
3.2	Analysis of Char	48
3.2.1	Effect of Heating Method	48
3.2.2	Effect of Potassium Loading.....	49
3.2.3	Effect of Temperature	50
3.3	Analysis of Gas.....	51
3.3.1	Effect of Heating Method	52
3.3.2	Effect of Potassium Loading.....	56
3.3.3	Effect of Temperature	60
3.4	Elemental Mass Balance.....	61
Chapter 4 CONCLUSIONS AND RECOMMENDATIONS.....		66
4.1	Conclusions.....	66
4.2	Recommendations for Future Work.....	67
References.....		68

List of Figures

Figure 1.1: Dipolar mechanism visualization	12
Figure 1.2: Sample temperature gradient comparison between conventional (left) and microwave heating (right)	14
Figure 1.3: Plots of mercury porosimetry for samples Vef and Vmw. Variation in the specific pore volume with pore diameter: accumulative volume (dots), derivative (lines)....	18
Figure 2.1: Schematic of microwave experiments.....	29
Figure 2.2: Schematic of electric furnace experiments.....	29
Figure 2.3: Picture of the quartz reactor used in all MWP experiments. The top and bottom parts of the reactor create an air tight seal through a ground quartz interface	30
Figure 2.4: Relationship between emissivity and sample temperature for various carbon based materials	33
Figure 2.5: Relationship of microwave input power versus pyrolysis temperature	34
Figure 2.6: Temperature profiles for MWP at 700 °C. a) S; b) K0.7; c) K3.5	37
Figure 2.7: Temperature profiles for MWP at 1000 °C. a) S; b) K0.7; c) K3.5	38
Figure 2.8: Temperature profiles of MWP carried out at 800 and 900 °C for K3.5.....	39
Figure 3.1: Product fractions versus potassium loading. a) CP at 700 °C; b) MWP at 700 °C; and c) MWP at 1000 °C	45
Figure 3.2: Product fractions versus temperature. a) is for S; b) is for K0.7; and c) is for K3.5	46
Figure 3.3: Proximate analysis results for char plotted against potassium and temperature. Ash values are displayed on a dry, K ₂ O free basis. The different plots are: a) CP at 700 C; b) MWP at 700 C; c) MWP at 1000 C; d) S MWP e) K0.7 MWP f) K3.5 MWP	50
Figure 3.4: Syngas production plotted against both potassium loading and temperature.	54
Figure 3.5: Product gas production versus potassium loading. a) CP at 700 °C; b) MWP at 700 °C; c) MWP at 1000 °C.....	58
Figure 3.6: Product gas composition versus potassium loading. a) CP at 700 °C; b) MWP at 700 °C; c) MWP at 1000 °C.....	59
Figure 3.7: Product gas volume versus temperature for MWP. a) S; b) K0.7; c) K3.5.....	63

Figure 3.8: Product gas composition versus temperature for MWP. a) S; b) K0.7; c) K3.5 64

List of Tables

Table 1.1: Ultimate analysis of biomass feedstock properties (values given in wt percent unless otherwise noted).....	4
Table 1.2: Biogas properties for various experiments (gases presented as vol %).....	5
Table 1.3: Bio-oil properties for various experiments (presented as wt percent).....	8
Table 1.4: Properties of pyrolytic char from various biomass feedstocks.....	19
Table 1.5: Functional groups and their associated decomposition temperature ranges.....	20
Table 2.1: Properties of corn stover samples.....	27
Table 2.2: Corn stover sample's ash composition (ug metal oxide/g dry corn stover).....	27
Table 2.3: Parameters to reach appropriate MWP temperatures.....	33
Table 3.1: Product Fraction Results (in weight % on ash free basis).....	43
Table 3.2: Properties of char produced in each experiment.....	49
Table 3.3: Gas production analysis for all experiments.....	53
Table 3.4: Stoichiometric calculations for pyrolysis reactions.....	56
Table 3.5: Volumetric calculations for pyrolysis reactions.....	56
Table 3.6: Elemental Product Distribution. (Error: wt. % of element found in all products subtracted from the wt. % of element found in original feedstock).....	65

Acknowledgements

I would first and foremost like to thank Dr. Sarma Pisupati for providing me guidance and support throughout my graduate experience. I would also like to thank Dr. Nandakumar Krishnamurthy for his support with my sample preparation and experimental setup questions, as they were some of the hardest questions to answer for this work. I cannot thank my thesis committee members, Dr. Dinesh Agrawal and Dr. Caroline Clifford, enough for their incite and unique perspectives that helped strengthen this work immensely. I would especially like to thank Dr. Dinesh Agrawal for the support in figuring out why my MWP temperature profiles were initially not reproducible.

This work would not have been possible without the timely, innovative, and meticulous glass blowing of Doug Smith. The quartz reactor used in this work was modified countless times for various reasons, and each time Doug worked on the reactor, he turned it into a new masterpiece. Although Doug recently retired, he is greatly missed by the faculty, staff, and students at Penn State.

I would also like to express gratitude for the privilege to work at The EMS Energy Institute. The instruments that were available for use were astounding both in numbers, and in quality. I would like to thank Ron Wasco for providing all of the instrument training, and general guidance. Working at the Material Research Laboratory's (MRL) Microwave Processing Center was also a great privilege. Their facility is world renown for their unique and numerous microwave configurations, and it was a great opportunity to operate their 6 kW multimode microwave. I want to thank Joe Kearns for providing all of the miscellaneous equipment that made this work possible, as well as working out a schedule for the microwave's usage. Also at the MRL, I have much appreciation for Jeff Long for his guidance about my conventional heating setup.

Inorganic analysis done in this study was carried out by Henry Gong, would I cannot thank enough for his quality analysis.

I need to thank Dr. Sarma Pisupati once again for providing me with financial support through a teaching assistanceship, through which I learned a lot. On this note, it is important that I also thank Dr. Tanya Furman for the financial support from my fellowship with the National Science

Foundation's Teaching Earth System Science Education (TESSE) program, which turned out to be an enjoyable learning experience for me.

I would like to thank my research group members for their incite and support throughout the past few years, namely: LaTosha, Nari, Ojogbane, Prabhat, Aime, Bob, Hari, Roshan, and Vasudev. The support from my family and friends is unbounded, and I cannot express enough appreciation for them. I would like to dedicate this thesis to my precious wife Lindsay, for all of her support and understanding during my time at Penn State University.

Chapter 1

INTRODUCTION

1.1 Motivation

At the turn of the twenty-first century, climate change became a hot topic in the mainstream media, and as a result, a worldwide concern arose about the possibility of human activity causing recent global temperatures to increase. This concern, coupled with fossil fuel resources becoming increasingly scarce, has caused a push for alternative energy research. The majority of recent research efforts involve renewable energy, as renewable energy will inevitably be the predominant energy source in the coming century. One well-known renewable energy source is biomass, and is currently the United States' largest renewable energy source.

Biomass production has the potential to produce 14 percent of the United States' electricity demand through a variety of available conversion methods [3]. Some available conversion methods include: anaerobic digestion, combustion, gasification, and pyrolysis. This study will focus on the pyrolysis conversion method, which is the thermal decomposition of organic matter in an oxygen-free environment. It has been demonstrated that combusting a bio-gas is typically a more efficient method to produce electricity than combusting the biomass itself, because scrubbing technologies are minimized in the former case [4]. Alongside this, the former case is a much cleaner way to produce electricity. This study chose pyrolysis over gasification because partial combustion of the biomass is not necessary in microwave pyrolysis, as the microwaves are providing and maintaining the high temperatures for conversion.

This work focuses on converting a biomass residue, corn stover, to produce a useful gaseous fuel. Corn stover is the portion of the corn plant that is left over after the corn has been harvested from the stalk. Corn stover was chosen because of its low ash content, which needed to be thoroughly removed by acid washing for this study. Different pyrolysis conditions determine whether bio-oil or biogas will be the major byproduct. This study's pyrolysis conditions are designed to maximize the biogas fraction, and more specifically, to produce a high

quality syngas consisting of mainly H_2 and CO . A syngas stream allows for efficient and clean electricity generation through a gas turbine.

It is anticipated in the future that commercial-scale biomass pyrolysis will require carbon capture technology. CO_2 separation requires the raw gas to be at a moderate temperature, so lower gas temperatures approaching the separation stage will require less of a temperature drop. For this reason, CO_2 separation is better implemented as a pre-combustion rather than a post-combustion method. Gas coming out of the gasifier would have to be cooled less for CO_2 separation compared to post-combustion. Pre-combustion CO_2 separation is made possible through a water-gas shift (WGS) reactor, in which virtually all the CO of the syngas reacts with steam, to generate CO_2 and H_2 . After this step, the CO_2 can be removed before combustion where there is negligible carbon to be converted into CO_2 . This is important to note because thermodynamically biogas with the highest possible calorific value (consisting mainly of hydrocarbons) is ideal for a gas turbine, but anticipated carbon capture requirements for commercial-scale pyrolysis plants favor a syngas.

A series of microwave-induced pyrolysis studies involving biomass have observed a trend of potassium rich biomass yielding a biogas with significant H_2 and CO content at the expense of CH_4 and CO_2 . When undergoing conventional pyrolysis, this potassium rich biomass did not convert nearly as much CH_4 and CO_2 to syngas. There is a clear discrepancy between potassium's affect on pyrolysis when dealing with these two heating methods [1, 5-7]. The objective to this work is to investigate the differing effects of potassium between conventional and microwave pyrolysis (CP and MWP, respectively).

MWP of biomass is feasible for a large scale continuously fed system; however, the process' energy requirement has not yet been compared to a conventional gasification process. This could be made by loading a microwave oven with a maximum amount of sample that allows for uniform sample heating. The same principle can be applied in a gasifier. Both the total energy requirement as well as the produced biogases' total theoretical energy can be obtained. These values can be turned into a net amount of energy per weight of biomass for both processing methods, and the process with the larger of these values can be considered the more efficient thermal conversion process.

1.2 Literature Review

1.2.1 Effect of Feedstock

It is important to gauge both the quantity and quality of fuel derived from corn stover compared to other pyrolysis feedstocks in order to know if corn stover pyrolysis is worth further investigation. In general, a quality fuel should have minimal sulfur, nitrogen and mutagenic constituents. A quality biogas consists of either a large calorific value, (i.e., large volume percentage of both H₂ and CO). Also, understanding the properties of the initial feedstocks will help to explain the cause of the varying fuel production results.

Compared to other forms of pyrolysis feedstock, corn stover's calorific value is most similar to urban sewage sludge (See *Table 1.1*). Corn stover's H/C atomic ratio is lower than most other pyrolysis feedstock types, which is generally not ideal for H₂ production [8].

Various types of biomass have been investigated for their potential as different feedstocks for fuel gas production, including dry and wet sewage sludge [8-10], a dry sewage sludge/manure mixture [11], dry microalgae [12, 13], coffee hulls [5] and mallee oil [14]. These studies' either focused on producing the greatest possible gas fraction [5, 8, 9, 11] or oil fraction [10, 12-14], but comparing their results will give a qualitative idea of best feedstock for each fuel type. All product fractions tabulated in this paper are presented as a weight percentage of the dry feedstock.

1.2.1.1 Biogas Optimization

Table 1.2 provides the biogas analysis of the previously discussed biomass pyrolysis studies. Unfortunately, the corn stover study did not analyze the gas constituents produced, so it is not known how biogas derived from corn stover compares with other feedstocks. It is clear that coffee hulls have the most optimal gas fraction, but it is necessary to look at the gas quality as well.

The coffee hulls study produced a gas made up of 40 percent H₂ and 72.9 percent synthesis gas (H₂ + CO); whereas typical urban sewage sludge had produced gas comprised of 32.8 percent

Table 1.1: Ultimate analysis of biomass feedstock properties (values given in wt percent unless otherwise noted)

Pyrolysis Feedstock	M	Ash ^a	VM ^a	FC ^{a,c}	Organic Fraction ^b						HHV ^a (kJ/kg)	Reference
					C	H	N	S	O ^c	H/C		
Urban SS	71.0	31.2	62.3	6.5	52.3	8.0	6.7	0.7	32.3	1.54	16,682	[8]
Anaerobically digested SS	81.0	38.1	54.7	7.2	49.1	7.3	8.1	1.5	34.0	1.78	14,032	[8]
CaO and FeCl ₃ stabilized SS	74.7	42.3	55.9	1.5	39.3	7.3	6.2	0.8	46.3	2.23	10,287	[8]
Milk derivative SS	84.3	17.6	73.2	9.2	47.8	6.7	9.0	1.2	35.4	1.68	18,104	[8]
Dry SS	5.6	28.4	70.7	0.9	54.6	8.2	7.4	1.1	27.8	1.77	15,220	[10]
SS/Manure Mixture	6.9	23.0	64.8	12.3	52.6	7.1	6.6	1.0	32.2	1.62	17,140	[11]
Pine	-	0.2	80.3	19.5	50.3	6.3	0.1	-	43.3	1.50	-	[14]
Oil Mallee	-	0.5	81.9	17.6	48.4	6.3	0.1	-	45.2	1.56	-	[14]
Corn Stover	-	6.8	75.6	17.6	41.9	5.3	-	-	46.0	1.52	16,540	[15]
Coffee Hulls	8.2	5.6	77.0	17.4	47.3	6.4	2.7	0.3	37.7	1.62	17,900	[6]

^a Dry basis

SS: Sewage Sludge

^b Dry and ash free basis

^c Calculated by difference

Table 1.2: Biogas properties for various experiments (gases presented as vol %)

Pyrolytic Bio-gas	Reactor Type	Product Fraction ^a	H ₂	CO	O ₂	N ₂	CH ₄	CO ₂	C ₂ H ₄	H ₂ + CO	H ₂ /CO	HHV (kJ/m ³)	Reference
Urban SS	MM	54.9	32.8	30.3	23.8	16.9	6.4	8.1	3.1	63.1	1.08	8,587	[8]
Urban SS	EF	61.0	29.1	16.2	3.0	14.6	18.6	11.5	6.2	45.3	1.50	13,855	[8]
Anaerobically digested SS	MM	43.2	32.2	30.6	3.5	24.0	4.6	3.8	1.0	62.8	1.05	6,903	[8]
CaO and FeCl ₃ stabilized SS	MM	46.2	42.8	23.2	3.8	24.7	1.4	3.6	1.3	66.0	1.54	6,607	[8]
Milk derivative SS	MM	57.3	21.6	26.6	3.9	27.0	6.9	11.4	2.7	48.2	0.81	7,168	[8]
SS and Manure Mixture	FB	39.0	28.1	20.5		3.5	22.0	14.8		48.6	1.37	24,300	[11]
Coffee Hulls	SM	68.7	40.1	32.8			6.8	17.7	2.2	72.9	1.22	15,500	[6]
Coffee Hulls	EF	66.6	29.9	23.1			10.7	32.1	2.9	53.0	1.29	12,700	[6]

MM: Multi-mode Microwave

SM: Single-mode Microwave

EF: Electric Furnace

FB: Fluidized Bed

SS: Sewage Sludge

^a Dry basis

H₂ and 63.1 percent synthesis gas, or syngas. Throughout this document, gas composition percentages are given on a volume basis. The higher heating value of the biogas produced from sewage sludge is significantly lower than that produced from coffee hulls. These calorific values show that there are larger volumes of energy dense gases in the coffee hull's biogas compared to the sewage sludge biogas.

When considering both the gas fraction percentage as well as the gas composition, it is evident that coffee hulls offer the most favorable H₂ and syngas production of the aforementioned biomass feedstocks. The coffee hulls study suggested this superb production of syngas was probably due to the feedstock's significant potassium content acting as a catalyst. The suggested catalytic reactions promoted by potassium are discussed later in this review.

1.2.1.2 Bio-oil Optimization

Table 1.3 provides a summary of the bio-oil fraction and composition data from the studies previously mentioned. All oil fraction percentages presented in this review are based on the calculated dry feedstock weight. Mallee oil and microalgae provide the largest oil fraction by far (nearly twice that of dry sewage sludge). It should be noted that the studies with the three highest oil fraction studies were all performed in fluidized bed reactors. More details about this reactor's pyrolytic behavior will be discussed in Section 3.

The calorific values of these oils shall be the main means to compare the bio-oils of various feedstocks, since the most feasible application for these highly-viscous bio-oils will be used in a combustion process. The heterotrophic microalgae produced the most energy dense bio-oil at 41 MJ/kg, followed by the wet sewage sludge's bio-oil at 36.8 MJ/kg, and the coffee hull's bio-oil was slightly less energy dense at 34 MJ/kg. For a rough idea of how these values compare to conventional fuel, fossil oil's calorific value is roughly 42 MJ/kg [12]. The majority of these presented bio-oils are highly viscous, which limit their types of applications. These bio-oils will definitely not be suitable as transportation fuels, but they are likely to be suitable for various heating applications.

Another issue that needs to be considered for the use of bio-oil as a fuel is its polycyclic aromatic hydrocarbon (PAH) content. PAHs have been shown to be mutagenic and/or carcinogenic [8]. The microalgae study showed an aromatic content of 2.2 percent, which can be assumed to

contain insignificant levels of PAH's. The mallee oil study also did not specifically address PAHs in its bio-oil analysis, leaving the bio-oil's safety in question. The oil mallee study did mention that their derived bio-oil was found to be highly viscous (due to lignin derived oligomers) under conditions to optimize the oil fraction, thus limiting the bio-oil's application to power generation and new material production.

Elevated nitrogen content is also an environmental concern with any combusted fuel due to NO_x formation at combustion temperatures. The nitrogen content of the bio-oils derived from autotrophic microalgae was the highest at 10 percent, coffee hulls and wet sewage sludge derived oils trailed closely behind, leaving heterotrophic microalgae and mallee oil the least NO_x forming oils. Any bio-oils with significant nitrogen content may require nitrogen removal.

It appears that although wet sewage sludge derived bio-oil has a larger calorific value than that of dry sewage sludge, the oil fraction percentages make dry sewage sludge the more optimal bio-oil feedstock. Overall, bio-oil derived from heterotrophic microalgae is the highest quality and nearly the largest quantity, making it the ideal bio-oil feedstock. Further analysis should be carried out on these aforementioned bio-oils' PAH content, which could seriously limit the bio-oil's applications.

1.2.1.3 Effect of Inherent/Added Catalysts

There have been quite a few thermal conversion studies introducing various metals as catalysts.

One study that looked at the pyrolysis of several types of biomass established that in general, inorganic-stripping increases the initial decomposition temperature and the weight loss rate of thermal-decomposition. Biomass with high lignin, K and Zn content, actually increase their char yield when stripped of their inorganic content. This suggests that K and Zn promote char heterogeneous reactions that would not otherwise occur. When comparing the catalytic effect of K and Zn, Zn impregnated biomass yielded significantly greater gas fractions with proportionately less char fractions than K impregnated biomass. Although this finding is important, Zn is found in significant amounts in only a handful of biomass species, rice husks being one of them. Potassium however, is abundant in almost all natural biomass feedstocks. For all biomass feedstocks, this study found that liquid yields increased at the expense of the gas yield for inorganic-free biomass, implying that inorganic constituents play an important role in

Table 1.3: Bio-oil properties for various experiments (presented as wt percent)

Pyrolytic Bio-oil	Reactor Type	Product Fraction ^a	C	H	N	S	O ^b	H/C	HHV (kJ/kg)	Reference
Typical urban SS	MM	10.3	73.5	8.5	6.2	-	11.5	1.39	36,813	[8]
Typical urban SS	EF	3.1	86.5	3.6	4.9	-	5.0	0.50	36,429	[8]
Anaerobically digested SS	MM	13.1	71.5	8.4	7.5	-	12.6	1.41	35,922	[8]
CaO and FeCl ₃ stabilized SS	MM	4.7	73.2	8.8	6.6	0.6	10.8	1.44	36,178	[8]
Milk derivative SS	MM	19.7	86.5	3.6	4.9	-	5.0	0.50	33,962	[8]
Dry SS	FB	52.0	36.3	9.8	7.6	0.7	45.7	3.23	23,330	[10]
Autotrophic Microalgae	FB	18.0	62.1	8.8	9.7	-	19.4	1.69	30,000	[13]
Heterotrophic Microalgae	FB	56.0	76.2	11.6	0.9	-	11.2	1.53	41,000	[13]
Coffee Hulls	SM	8.6	74.4	8.2	8.0	0.6	8.8	1.32	34,000	[6]
Coffee Hulls	EF	9.8	70.5	8.1	8.1	0.6	12.7	1.38	30,600	[6]
Oil Mallee	FB	75.8	52.0	7.0	0.1	-	42.0	1.62	21,300	[14]
Birch	FB	-	44.0	6.9	0.1	-	49.0	1.58	16,500	[16]
Pine	FB	-	45.7	7.0	0.1	-	47.0	1.54	17,200	[16]
Poplar	FB	-	48.1	5.3	0.1	-	46.1	1.32	17,300	[16]
Reference Fuels										
Block wood	-	-	46.9	6.1	1.0	0.0	44.0	1.55	18,300	[17]
Low ranked coal	-	-	62.1	6.1	1.1	1.9	28.8	1.18	13,500	[18]
High ranked coal	-	-	82.6	3.0	0.9	0.7	3.7	0.44	33,000	[19]
Fossil oil	-	-	83.0 - 87.0	10.0 - 14.0	0.1 - 0.7	0.1 - 5.0	0.1 - 1.5	1.69	42,000	[13]

MM: Multi-mode Microwave

SM: Single-mode Microwave

EF: Electric Furnace

FB: Fluidized Bed

SS: Sewage Sludge

^a Dry basis

^b Calculated by difference

promoting secondary cracking reactions during pyrolysis [20].

Although this deashing study tells a large portion of the effect of inorganic contents on pyrolytic behavior, it fails to tell specifically which reactions are being promoted by K and Zn, which is important for understanding mechanisms involved in pyrolysis.

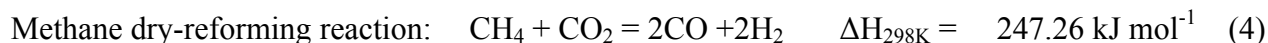
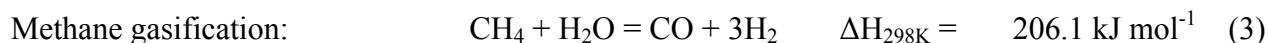
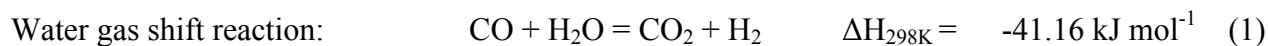
A gasification study looking at the influence of alkaline earth metals such as calcium, strontium and barium found that coal char's gasification rates were increased in the following manner: $\text{Ca} < \text{Sr} < \text{Ba}$. The demonstrated catalysis is not from lowering the char's true activation energy, but instead through the densification of reaction sites. Intriguingly, an addition of 0.3 wt. percent of barium caused the gasification rate to increase by over two orders of magnitude [21].

A similar study looked at several various catalysts in coal gasification with different reactant gases (steam and CO_2 and H_2). It was found that reactant gases largely determine the activity of the catalysts. For steam, the order of increasing activity is: coal ash $< \text{Fe} < \text{Ni} < \text{Ba} < \text{K}$. Barium ranked similarly in the previously discussed study as a steam gasification catalyst, just below potassium. In CO_2 and H_2 gasification, the order of increasing activity is: coal ash $< \text{Ba} < \text{K} < \text{Fe} < \text{Ni}$. The catalytic effect of potassium in steam gasification has been extensively documented, and many theories exist on its catalytic mechanisms [22].

A catalysis study of Ni-Al formulation with Ca and/or K has been demonstrated to promote the water-gas shift conversion to produce syngas in gasification [23]. Most of these catalytic studies were kinetics based analyses, and did not provide any analysis on the gas composition produced from these various catalysts.

One study was carried out on the reforming of CO_2 and CH_4 using a potassium rich char to serve as a catalyst during MWP [24]. The purpose of the study was to gain further understanding of the reactions taking place during coffee hull MWP, which has produced the most optimal gas of the studies discussed in this review. CO_2 and CH_4 were introduced to a char catalyst and the reverse of reaction (1) followed by reaction (3) occurred continuously until the catalyst was spent. Reactions (1) and (3) combined produce reaction (4). Furthermore, CH_4 would react with the char catalyst to generate hydrogen and a char solid (reverse of reaction (2)). The CO_2 in the reactor also regenerated the char catalyst by reaction (5). The more CO_2 available to rejuvenate the catalyst, the more reforming of CO_2 and CH_4 was able to take place. When optimizing the

CO₂ input flow, the product gas was a syngas with virtually no CO₂ or CH₄. These reactions were evident in CP, but were not as prominent as in MWP.

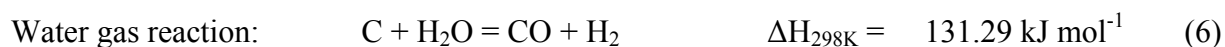


The study discussed above provides compelling evidence that MWP enhances catalytic activity, but does not demonstrate for certain which catalyst is enhanced in microwave heating. Potassium is a well known catalyst in the thermal conversion of materials [20, 25-30], and it is the likely culprit, but several catalysts in the char bed could have played an active role in this study. It is for this reason that this work focuses on the effect of potassium under CP and MWP.

1.2.1.4 Effect of Moisture Content

All wet sewage sludge described in the aforementioned literature have moisture contents between 70 to 82 percent. This is important to recall when studies are done with dry sewage sludge because of the large energy requirement for removing the bulk moisture before pyrolysis can occur.

Moisture content has been addressed in two studies involving sewage sludge pyrolysis [1, 31]. Dominguez *et. al.* (2006) found that as moisture content increases, the gas fraction increases at the expense of the char fraction. More specifically, as moisture content increases, H₂, CO₂, and C₂H₄ increase while CO, CH₄, and C₂H₆ decrease in the gas fraction. The increase in H₂ and CO₂ as well as the decrease in CO can be explained by the water gas shift reaction. A higher moisture content will increase the water vapor released during pyrolysis temperatures, and will thus promote the water gas shift reaction. Reaction (6) shows how carbon monoxide is formed during pyrolysis and reaction (1) shows how it is then converted into carbon dioxide through secondary reactions.



Dominguez *et. al.* (2006) also noted that there was a different evolution of species in low temperature ranges between wet and dry sewage sludge pyrolysis. With wet sewage sludge, there were substantial percentages of H_2 , CO and CH_4 in the 250-400 °C sample temperature range, and there were non-detectible levels observed with dry sludge in this temperature range. This suggests that steam (from wet sewage sludge) reacts with intermediate products generated at the beginning of the pyrolysis reactions. The long gas residence time inside the reactor promoted reaction (1) before all the steam left the reactor. A short residence time would have most likely resulted in a noticeably larger aqueous portion of the liquid fraction.

Dominguez *et. al.*'s 2008 study demonstrated inconsistent behavior with varied moisture contents between MWP and CP, so it was rather difficult to identify significant behavior from this study. The single apparent finding relating to moisture content is that dry sewage sludge created more CO in the gas fraction than wet sewage sludge. An observed behavior that was worth noting is that when pyrolysis was carried out in microwaves, increased moisture caused the gas fraction to decrease. The inverse was true for pyrolysis in an electric furnace. This discrepancy might be due to the effect of microwave drying compared to conventional drying before CP was carried out. It was found that microwave drying creates a larger pore volume than conventional drying. A larger pore volume allows volatiles to be released with little physical resistance, making it less likely for secondary reactions to occur, and thus releasing larger hydrocarbons. In CP, the pore volume is a lot smaller, creating more physical resistance for the emitted volatiles. More resistance could equate to longer residence times of the volatiles within the sample itself, which would promote secondary reactions, and therefore a larger gas fraction [32].

1.2.2 Effect of Reactor Type

Pyrolysis has been carried out using various heating methods. One study carried out pyrolysis experiments in a rotary-kiln reactor [33]. Several pyrolysis studies have utilized a fluidized bed reactor for optimizing oil production [10-12, 14, 34]. The majority of microwave pyrolysis studies involve sewage sludge [1, 5, 8, 9, 35-38]. This is probably due to the fact that sewage

sludge contains substantial moisture, and microwave heating is one of the most energy efficient ways to remove moisture pre-pyrolysis.

1.2.2.1 Microwave Heating Theory

Microwaves heat objects by three main mechanisms: dipolar, conduction and magnetic losses [39]. In the dipolar mechanism (see *Figure 1.1*), microwaves excite *dielectric (polarized) molecules* contained within the object by continually changing the electromagnetic field inside the object. The dielectric molecules adjust to this changing electromagnetic field that is induced by the passing microwave. When exposed to passing microwaves over time, the movement of the dielectric molecules creates friction inside the object, and the object heats up. The conduction mechanism involves charge carriers (i.e. electrons or ions) moving through *conductive materials* with the changing electromagnetic field which results resistive heating. It should be noted that metallic conductors reflect microwaves, so they typically are not suitable for microwave heating. Magnetic losses of a material such as eddy current losses, hysteresis losses, as well as domain wall losses induce heating under microwave exposure [39].

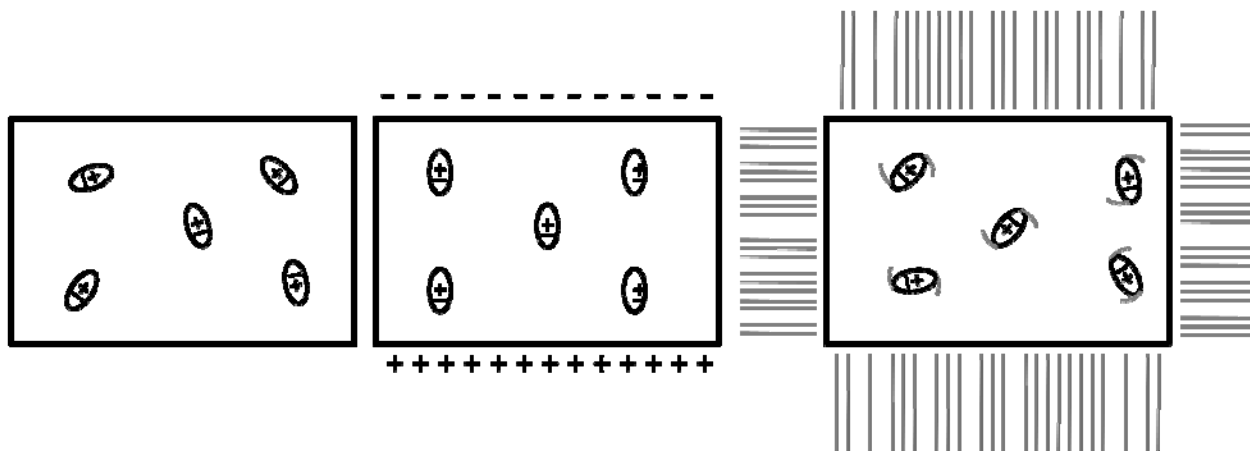


Figure 1.1: Dipolar mechanism visualization

The formula for the power absorbed from a specific material exposed to microwaves is given below. The former term of this equation provides the power being absorbed by insulator materials, and the latter term provides the absorbed power of conductive materials. Properties produced from the microwave are the microwave frequency (ω), the intensity of the electric field

(E), and the intensity of the magnetic field (H). The material properties that influence the power absorbed are the dielectric losses (ϵ''), the magnetic losses (μ''). Properties of the medium through which the microwaves propagate, such as permittivity of free space (ϵ_0) and permeability of free space (μ_0) also affect the absorbed power.

$$P = \omega[\epsilon_0\epsilon'' E^2 + \mu_0\mu'' H^2]$$

P = Power absorbed

ω = Frequency ($2\pi f$)

ϵ_0 = Permittivity of free space

ϵ'' = Dielectric loss factor

E = Intensity of electric field

μ_0 = Permeability of free space

μ'' = Magnetic loss factor

H = Intensity of magnetic field

A high temperature microwave heating study has identified a phenomenon produced by microwaves, which has never before been achieved [2]. The phenomenon described was anisothermal heating within samples (significant temperature gradients on a localized level.) This anisothermal situation created in microwave heating is seen when a sample contains at least two types of material. At least one of these materials is an excellent microwave absorber, and the other materials are not strong microwave absorbers. This anisothermal situation has been demonstrated to induce reactions much more rapidly than in solid-state, isothermal conditions created in conventional heating. It has been demonstrated that the hotter species diffuses to the relatively cooler species, greatly increasing reaction rates [2]. This phenomenon may actually increase certain pyrolysis reactions to increase syngas production in microwave pyrolysis.

When being microwaved alone, biomass does not exceed 200 °C because that is the temperature the biomass's internal moisture (water is a polarized molecule) reaches before it leaves as steam, and nothing else in biomass couples with microwaves at 200 °C [38]. Due to this phenomenon, biomass requires a proper microwave receptor to reach pyrolytic temperatures (greater than 340 °C). Options for such receptors include pyrolytic char, graphite, or metal oxides [38]. Once the

sample is dried, and passes 340 °C with the help of the microwave receptor, the sample begins pyrolyzing, slowly producing char. The char that is created from pyrolysis then begins to couple and absorb the microwave energy, after which the sample temperature rises at an impressive heating rate. The heating rates demonstrated from MWP have more than doubled the heating rate provided by CP [8]. This equates to shorter processing times for MWP, which is attractive from both energy conservation and economic perspectives.

Notice in *Figure 1.2* the different sample temperature gradients in conventional heating and microwave heating. Because microwaves heat samples directly, instead of transferring heat across a medium, samples are hottest in their center and coolest on its outside surface due to heat loss to its surroundings. This heating profile is opposite that of conventional heating, where the sample's surroundings are the hottest, so the outside of the sample is hottest, and the center of the sample is coolest. In general, microwaves provide the following advantages over conventional heating methods: significantly reduced operating times which equates to energy savings, increased heating efficiency, material selective heating, greater heating control, and reduced size/complexity of the heating equipment [40].

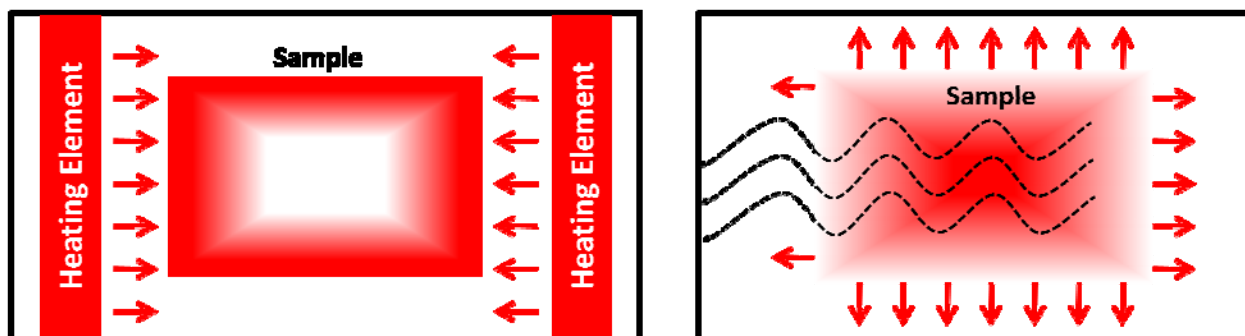


Figure 1.2: Sample temperature gradient comparison between conventional (left) and microwave heating (right)

1.2.2.2 Biogas Optimization

Based on the fact that fluidized bed reactors have been used in several studies to maximize the bio-oil fraction, a biogas produced in a fluidized bed reactor is anticipated to have more energy dense hydrocarbons, which is the case as shown in *Table 1.2*. Though the gas fraction is not as

large as that produced by other reactor types, the gas produced has substantially higher energy higher heating value (HHV).

In general, electric furnace pyrolysis of sewage sludge yields a slightly larger gas fraction compared to MWP. Dominguez and Menendez believe this is due to the fact that in conventional heating, the reactor wall temperatures are high and the sample's temperature is relatively low, creating longer gas residence times near the sample, and thus promoting secondary reactions. The inverse of this could explain the MWP results because the reactor wall is transparent to microwave energy, but the sample is not [9, 36]. The discrepancy in the gas fraction between the two heating methods is more likely to be explained by a study that looked at the effect of microwave drying compared to conventional drying before CP was carried out. It was found that microwave drying of biomass creates a sample BET surface area more than 5 times greater than conventional drying. This large surface area was due to an elaborate pore structure caused by the rapid evaporation of water during microwave heating. These relatively elaborate pore networks will give released volatiles shorter residence times within the sample, making it less likely for secondary cracking reactions to occur. In CP, the pore volume is a lot smaller, creating more physical resistance for the emitted volatiles. More resistance equates to longer residence times of the volatiles within the sample itself, which would promote secondary reactions, and therefore a larger gas fraction at the expense of the oil fraction [32].

Dominguez *et. al.* has also demonstrated the opposite trend by producing 11 percent more sewage sludge derived gas in microwave experiments than conventional experiments [1]. The coffee hull study produced a much larger gas fraction with MWP compared to electric furnace pyrolysis [5]. This suggests that the properties of the biomass feedstock are more indicative of the gas fraction results. The electric furnace pyrolytic gas typically has a larger calorific value (13.9 MJ/m^3) compared to microwave pyrolytic gas (8.3 MJ/m^3). This insinuates that CP contains a greater hydrocarbon gas makeup than the microwave pyrolytic gas, which has a higher concentration of syngas. The advantages and disadvantages of these gases' applications are discussed in detail in the *Introduction*.

Hydrogasification is evident in electric furnace pyrolysis because there is a lower aqueous fraction and larger gas fraction compared to MWP. CP also produced elevated CO_2 in the biogas via reaction (1) [5, 36]. The Boudouard reaction has been shown to be favored during MWP

more than electric furnace pyrolysis because of elevated CO at the expense of CO₂, and a decreased char fraction in MWP. In this reaction, the CO₂ produced from pyrolysis reacts with the char in a gasification reaction to produce CO, which fits the presented results. Dominguez *et al.* also produced decreased concentrations of CO₂ in both their 2007 and 2008 studies [1, 5]. Their 2007 study produced decreased concentrations of CH₄ (50 percent and 70 percent, respectively) for MWP compared to CP. The reverse methanation reaction can explain the minute CH₄ content in MWP biogas.



A study looking at CO₂ and CH₄ reforming found that microwave heating demonstrated greater conversion of CO₂ and CH₄ into syngas compared to electric furnace heating. This study suggested that micro-plasma was observed around potassium in the char in the case of MWP. This micro-plasma phenomenon could be a part of the explanation of the discrepancy between the two heating method types [24].

1.2.2.3 Bio-oil Optimization

It is clear from the number of fluidized bed reactor studies with oil optimization goals that the fluidized bed reactor has great potential for bio-oil production compared to other methods of heating. Looking at the oil fractions of different methods will make this point clear. The oil fractions resulting from sewage sludge studies demonstrated 30 percent in a fluidized bed reactor [34], 10 percent in a microwave, and 3 percent in an electric furnace [8]. It is apparent that MWP produces three times more oil compared to electric furnace pyrolysis. It is worth mentioning that the fluidized bed study used dry sewage sludge, as wet sewage sludge would inhibit the gas flow required to make the sewage sludge behave like a fluid. The process of drying sewage sludge can be very energy intensive with conventional heating methods, and may not be practical for certain wastewater treatment facilities. The calorific values of the microwave and electric furnace bio-oils average out to be similar [8]. Bio-oils from MWP have been observed to be more aliphatic and oxygenated compared to electric furnace pyrolysis [35].

As previously stated, PAHs can be problematic for certain heating methods and should be carefully monitored. The fluidized bed study mentioned a large aromatic content in the sewage

sludge bio-oil but did not specifically address the PAH content in the bio-oil. In the case of sewage sludge pyrolysis, electric furnace heating has consistently formed small oil fractions, consisting largely of PAHs. For the MWP of sewage sludge, aromatization is not great enough to produce significant amounts of PAHs.

When studying coffee hull pyrolysis in 2007, Dominguez *et. al.* showed that MWP produced a bio-oil with slightly higher nitrogen content than that for electric furnace pyrolysis. The opposite behavior has been observed consistently when pyrolyzing sewage sludge [8, 35]

1.2.2.4 Char Optimization

Although pyrolytic char is generally assumed to be a waste stream from the pyrolysis process, its properties can help tell how complete pyrolysis conversion was, as well as which elements were not decomposed in the process, etc. A summary of various studies char properties is presented in *Table 1.4*.

There was negligible difference found in the chars' weights produced between MWP and electric furnace pyrolysis of sewage sludge in several studies [9, 35, 36]. Dominguez *et. al.* has produced slightly different results more recently, producing 13 percent less char mass in MWP than electric furnace pyrolysis [1].

A char leaching study showed that char produced from a microwave was less porous than conventional char (see *Figure 1.3*), causing less metals to leech from the microwave char [36]. Comparing this finding to the previously discussed microwave drying study [32], there are seemingly conflicting porosity trends in these findings that need to be explained. Looking at MWP holistically, it is possible that the porosity of a sample changes drastically between the drying stage and the end of MWP. It is likely that the drying step develops large pore networks, causing low gas residence times within the sample, thus reducing cracking reactions in the early stages of MWP. Toward the later part of pyrolysis when the sample temperature is high, internal hotspots produced in the microwave process could be causing the remaining carbon in the char to sinter into a glassy like matrix, which encases the internal metal content.

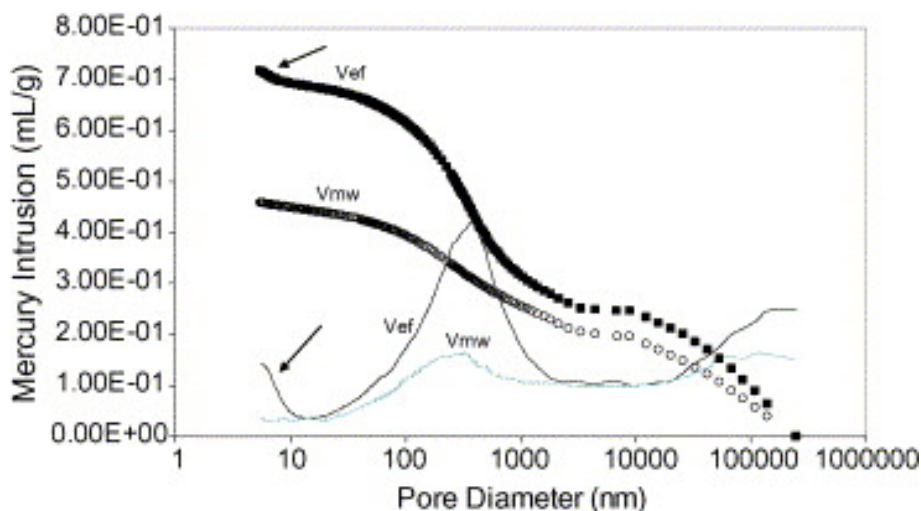


Figure 1.3: Plots of mercury porosimetry for samples Vef and Vmw. Variation in the specific pore volume with pore diameter: accumulative volume (dots), derivative (lines)

Source: Menendez, J.A., et al., *Microwave-induced drying, pyrolysis and gasification (MWDPG) of sewage sludge: Vitrification of the solid residue*. *Journal of Analytical and Applied Pyrolysis*, 2005. 74(1-2): p. 406-412.

1.2.3 Effect of Operating Conditions

Maximizing a specific product fraction is possible by adjusting the following operating conditions: pyrolysis temperature, heating rate and residence time. Shen *et al.* studied the operating conditions necessary to maximize the oil fraction [34], while Dominguez *et al.* [31] and Sanchez *et al.* [11] studied the operating conditions that maximize the gas fraction. Savova *et al.* looked at pyrolyzing biomass to create a char suitable for adsorption, and found that the char fraction is increased with low temperatures and low heating rates [41].

1.2.3.1 Pyrolysis Temperature

Ischia *et al.* developed a mass loss curve plotted against pyrolysis temperature. The curve consisted of two main events; the first event was when the fastest mass degradation occurred when sample temperatures reached 100 to 600 °C, losing half of its initial dry weight. The second event was a more gradual degradation occurring from sample temperatures of 600 to 1000 °C, where another 10 percent of the sample's initial dry mass was lost [42]. The greatest mass loss during mallee oil pyrolysis occurred when the sample temperatures were between 250 and 450 °C [14], which is similar behavior shown by Ischia *et al.* These mass losses plotted against temperature correlate well with *Table 1.7*, which suggests that during various

Table 1.4: Properties of pyrolytic char from various biomass feedstocks

Pyrolytic Char	Reactor Type	Product Fraction ^a	M	Ash ^a	VM ^a	FC ^c	Organic Fraction ^b					HHV ^a (kJ/kg)	Reference
							C	H	N	S	O ^c		
Typical urban SS	MM	34.8	0.4	82.5	3.6	13.5	92.4	2.3	3.5	1.9	0.0	5,576	[9]
Typical urban SS	EF	35.9	0.6	80.0	5.0	14.4	88.1	3.1	4.6	2.0	2.2	6,207	[9]
Dry SS	FBR	41.0	-	75.1	-	-	65.6	4.3	8.3	1.7	20.1	9,500	[10]
SS and Manure Mixture	FBR	39.0	3.4	57.9	8.6	33.5	90.4	1.4	6.0	1.2	1.1	13,710	[11]
Coffee Hulls	SM	22.7	-	23.9	18.6	57.5	69.6	0.9	2.6	0.4	2.6	23,400	[6]
Coffee Hulls	EF	23.6	-	24.4	12.3	63.3	69.3	0.7	1.6	0.3	3.7	24,000	[6]

MM: Multi-mode Microwave

SM: Single-mode Microwave

EF: Electric Furnace

FB: Fluidized Bed

SS: Sewage Sludge

^a Dry basis^b Dry and ash free basis^c Calculated by difference

temperature ranges certain functional groups will decompose. In the range 600 to 1000 °C, it is apparent that the weight loss observed is due to the decomposition of compounds containing significant amounts of oxygen.

Table 1.5: Functional groups and their associated decomposition temperature ranges

Source: Shen, L. and D.K. Zhang, *An experimental study of oil recovery from sewage sludge by low-temperature pyrolysis in a fluidized-bed. Fuel, 2003. 82*

Groups of Compounds	Temperature Range (°C)
Moisture	up to 150
Carboxylic	150 - 600
Phenolic	300 - 600
Ether oxygen	up to 600
Cellulosic	up to 650
Oxygen containing compounds	150 - 900

It was found in the studies comparing sewage sludge pyrolysis using microwave heating and conventional heating that microwave heating consistently achieve heating rates of 200 °C/min compared to 72 °C/min for conventional heating. This suggests that a microwave is over twice as fast in heating a saturated sample to a given temperature, providing greatly reduced reaction times. For MWP of sewage sludge, it took typically five minutes to obtain a temperature of 1000 °C, and usually required one minute soaking before there is no observable volatiles. This can be compared to CP of sewage sludge, which takes 14 minutes to heat the sample up to 1000 °C, and required 10 minutes soaking before pyrolysis completed. These results demonstrate that MWP was four times faster than electric furnace pyrolysis. This time savings translates into a decreased energy input for the pyrolysis process [37]. The main reason for the pyrolysis time discrepancy is microwave energy directly interacts with the moisture and evaporates it quickly compared to conventional heating which requires much more energy to internally dry the sewage sludge before pyrolysis can take place.

Particulates are a major cause for concern among thermal conversion processes and it should be noted that it is widely expected that in sewage sludge pyrolysis, no mineral ash is released at temperatures below 1200 °C [43], and none of the pyrolysis studies discussed within this work have exceeded that temperature.

1.2.3.2 Biogas Optimization

In general, higher temperatures yield larger gas fractions for biomass [8]. More specifically, when pyrolyzing coffee hulls, a gas fraction increase of 7 percent was observed when experiments with a peak temperature of 500 °C were compared with peak temperature experiments of 1000 °C [5]. High temperatures and long residence times encourage secondary cracking reactions to take place, creating a H₂ rich biogas [44]. It was also shown in coffee hull pyrolysis that increased temperatures increase the gas fraction at the expense of the char fraction, leaving the oil fraction constant with temperature. This suggests that heterogeneous reactions are promoted at higher temperatures. In the same coffee hull pyrolysis study, biogas calorific values were found to increase as pyrolysis temperature increases.

Hydrogen production is optimized with high heating rates and elongated residence times, so that steam, volatiles and char react at an elevated temperature before exiting the reactor [45].

1.2.3.3 Bio-oil Optimization

Shen *et. al.* found that oil production from sewage sludge pyrolysis is maximized at temperatures near 525 °C [34]. Garcia-Perez *et. al.* found that when pyrolyzing oil mallee, the bio-oil yield is maximized between 450 and 475 °C [14]. Acikogoz *et. al.* established an optimal temperature of about 500 °C when maximizing bio-oil from fast pyrolysis [46]. 450 °C was also the optimal temperature for maximizing microalgae's oil fraction [12]. Other studies focused on maximizing oil production carried out flash pyrolysis in the range of 400 to 600 °C [11, 12], fitting well with the optimal temperatures mentioned above.

Bio-oil produced from higher reaction temperatures contains increased portions of PAHs [8, 10]. This increasing PAH content can be explained by the pyrolysis behavior of polyolefins. When polyolefins are pyrolyzed at temperatures greater than 600 °C, aromatics are typically produced via the Diels-Alder reaction, which is a conjugated diene reacting with a substituted alkene. Another reason for abundant aromatic content at higher temperatures could be from the cracking of long-chain hydrocarbons [10].

Oil production is maximized with high heating rates and short residence times. It is also evident that when reactor temperatures exceed 450 °C, secondary reactions are promoted when residence

times are increased because light oil fractions have been shown to increase significantly as heavy oils decrease at pyrolysis temperatures above 450 °C [34].

1.2.3.4 Reactor Scaling

Scaling up reactors is another aspect of operation where some product differences arise. The sewage sludge and manure mixture study compared products on the laboratory scale to a products resulting from a pilot scale pyrolysis reactor. The pilot reactor yielded 5 percent less of a char fraction than the laboratory reactor. The pilot reactor did not produce any detectable oil fraction, so its gas fraction was very high at 66 percent, compared to the laboratory reactor's 27 percent. Following intuition, the calorific value of the pilot gas was found to be slightly lower than that of the laboratory gas, 23.8 compared to 24.3 MJ/m³, respectively.

1.2.4 Effect of Microwaving Conditions

MWP is not a new idea, and has been studied with sewage sludge [9], coffee hulls [1], corn stover [47], wood [17], and oil shale [48]. In general, microwaves provide the following advantages over conventional heating methods: significantly reduced operating times, increased heating efficiency, selective heating of materials, and reduced size/complexity of the heating equipment [40].

A study looking at different microwave ovens and receptor combinations was done in order to find the most optimal microwave heating configuration. A multimode oven utilizing graphite as a receptor produced the largest syngas volume, and second largest hydrogen volume. It yielded 66 percent greater syngas volume production compared to the worst experimental combination of single-mode oven using graphite as a receptor. The most hydrogen was produced using a combination of a single-mode oven utilizing char as a receptor. This setup also produced the second largest syngas volume [31]. The summary of this study would be that graphite is potentially the best receptor in a multimode oven if syngas production is the main goal, and when using a single mode oven, char is the best receptor for producing the most hydrogen.

Qualitative oil composition is the same regardless of the type of receptor used. When the graphite receptor is used, more 1-alkenes are produced than n-alkanes, suggesting that graphite catalyzes large aliphatic chain cracking into this lighter species.

1.2.5 Conclusion and Recommendations

Biomass pyrolysis has proven to produce a syngas rich biogas in MWP and CP utilizing high temperatures, and long gas residence times. MWP of coffee hulls produced the greatest amount of syngas in all of the studies discussed previously. The author of the coffee hulls study proved that microwaves enhanced coffee hull pyrolysis, and suggested that microwaves improved the coffee hull's inherent metal's catalytic effect of dry reforming methane (reaction (4)) into syngas.

Fluidized bed pyrolysis has proven to obtain the greatest bio-oil yield by operating around 500 °C, and using shortened residence times. PAH content in bio-oil is a relevant safety issue of bio-oil, and should be reported in future bio-oil production studies. Microalgae has demonstrated the largest bio-oil yield of all feedstocks discussed in this review, as well as the most energy dense bio-oil. Therefore, microalgae is a great renewable feedstock for the production of energy dense bio-oil.

MWP of biomass is feasible for a large scale continuously fed system; however, the process' energy requirement has not yet been compared to a conventional gasification process (currently considered the most efficient conventional way to produce power [4]). This could be made by loading a microwave with the maximum amount of sample that allows for uniform sample heating by applying the same principle in a gasifier. Collect both the total energy requirement as well as the produced biogases' total theoretical energy. These values can be turned into a net amount of energy per weight of biomass for both processing methods, and the larger of these values can be considered the more efficient thermal conversion process.

1.3 Problem Statement

The diminishing supply of dirty fossil fuels has pushed research efforts to find alternative fuel technologies. Pyrolysis of biomass has become a popular research focus because of its potential as a clean fuel/electricity producer. Microwave-induced pyrolysis of biomass is an attractive alternative to CP because of its significantly shorter processing time, which equates to lower energy requirements.

Previous pyrolysis studies have suggested that potassium content within biomass catalyzes the dry-reforming of methane. The objective of this work is to quantify potassium content's promotion of the dry-reforming reaction of methane in both MWP and CP. MWP temperatures of 700, 800, 900, 1000 and 1100 °C were investigated with potassium rich corn stover to investigate the temperature that best promotes potassium's catalytic behavior.

1.4 Hypothesis

It is anticipated that potassium will promote the dry-reforming of methane reaction to yield larger H₂ and CO gas volumes at the expense of CO₂ and CH₄, and that its catalytic effect will be more pronounced for MWP compared to CP. MWP will increase the catalytic effect of potassium because potassium is a metal that will, at high temperature, become a good microwave absorber [39]. The potassium will then create an anisothermal condition within the biomass sample, enhancing potassium's effect on pyrolysis reactions. This anticipation is based on a series of studies focusing on pyrolyzing potassium rich (2 percent dry basis) coffee hulls [1, 5, 24, 49, 50]. These studies proved that pyrolyzing coffee hulls produced an abundant amount of H₂ and CO rich bio-gas due to the coffee hulls promotion of the methane decomposition reaction (reverse of reaction 2), followed by the Boudouard reaction (reaction 5), the latter reaction actually rejuvenated catalyst sites for further reaction promotion. These studies also showed that these reactions were significantly increased in the case of MWP compared to CP.

1.5 Research Objectives

The goal of this study is to quantify the extent of potassium's catalytic effect for both CP and MWP. Comparing the difference in catalytic effect will lead to a greater understanding about the influence of microwaves on biomass' inherent catalytic ash content. Quantifying potassium's specific influence during MWP will also give an idea about how much H₂ and CO to expect from pyrolyzing potassium rich waste feedstocks such as coffee hulls, coir pith, ground nut shell, rice husks, and wheat straw in a microwave.

It was well established in other studies that temperature has a huge impact on biogas production, so for MWP, potassium's influence on pyrolysis will be compared to pyrolysis temperature's influence to see which has the most substantial effect.

The final goal of this study was to find the temperature that optimizes potassium's catalytic effect in MWP.

Chapter 2

METHODOLOGY

2.1 Corn Stover Preparation

The corn stover used in this investigation was provided by a corn farm in Bellefonte, Pennsylvania. The stover was peeled into less than 6 inch strands that fit into a blender to be blended. The stover was then dried in an air drying oven and then blended again. This drying and blending was carried out one additional time to provide a reasonable particle size of less than two mm.

After an appropriate particle size was reached, the corn stover was subjected to a hydrochloric acid wash, to remove the stover's inherent catalytic metal content. A 2M HCl solution (10 mL/g dry sludge) was prepared, and the corn stover was then poured into the solution. The acidic stover solution was continuously mixed and held at 60 °C for 6 hours. The solution was removed from heat for 48 hours to ensure the solution had sufficiently been absorbed by the corn stover. The mix was then held at 60 °C again for 6 hours. The solution was removed from heat, and filtered using a Buchner filter funnel and filter paper (Whatman 597) under vacuum conditions. The corn stover was rinsed with distilled water until filtrate reached a pH of about 7. This acid wash removed the inorganic constituents that were present as carbonates [51]. One quarter of this rinsed corn stover went into a drying oven for 48 hours, and was blended. This drying-blending process was carried out twice because of the particles tendency to clump together after the rinsing process, and then stored in air tight containers stored in a desiccator. This quarter of the stover will be referred to as metal-stripped corn stover, or S.

Another one quarter of the rinsed corn stover was mixed into a 0.07 M KOH solution. The last half of the rinsed corn stover was mixed into a 0.15 M KOH solution. These two mixes were left to soak for 48 hours to ensure the solution was internally absorbed by the particles. The mix was then filtered and rinsed a few times to remove the external solution. The samples were then oven dried, and processed like the case for sample S, described previously. The corn stover mixed in

the 0.07 M KOH solution ended up with a potassium content of 0.7 percent (dry basis), and will be referred to as K0.7. The corn stover mixed in the 0.15 M KOH solution ended up with a potassium content of 3.5 percent (dry basis), and will be referred to as K3.5. Intraparticle potassium distribution was not investigated, so potassium isn't necessarily uniformly distributed throughout sample material.

The properties of the sample types used in this investigation are given in *Table 2.1*. All sample types were characterized using a LECO 701 thermo-gravimetric analyzer (TGA) for proximate analysis, a LECO TruSpec CHN analyzer for elemental analysis, a LECO SC-144DR sulfur analyzer of sample, and a Par 1241 oxygen bomb calorimeter for the samples' higher heating values (HHV). The ash generated from the TGA was analyzed using a Perkin-Elmer Optima 5300 inductively coupled plasma atomic emission spectrometer (ICP) to get the composition of each sample's inorganic content, which is presented in *Table 2.2*.

Table 2.1: Properties of corn stover samples

	Moisture	VM	Ash	FC ^c	Organic Fraction ^b						HHV ^a (MJ/kg)
					C	H	N	S	O ^c	H/C	
CS	5.8	69.6	5.2	19.4	48.1	5.9	0.2	-	45.8	1.5	16.8
S	5.5	77.4	1.1	16.0	49.2	6.0	0.3	-	44.5	1.5	18.2
K0.7	5.4	68.3	2.7	23.6	53.3	5.9	0.6	-	40.2	1.3	19.6
K3.5	7.6	67.8	6.1	18.5	49.0	5.7	0.3	0.1	44.9	1.4	17.0

CS: Corn stover (as received)

^a Dry basis

^b Dry, ash free basis

^c Calculated by difference

Table 2.2: Corn stover sample's ash composition (ug metal oxide/g dry corn stover)

	Al ₂ O ₃	BaO	CaO	Fe ₂ O ₃	K0.7O	MgO	MnO	Na ₂ O	P ₂ O ₅	SiO ₂	SrO	TiO ₂
CS	1,311	< .01	6,560	740	2,613	9,873	15	8,761	4,872	14,357	2,836	71
S	869	5	68	54	1,244	136	< .01	24	102	9,470	2	26
K0.7	672	6	144	119	8,529	197	< .01	358	69	18,317	< .01	39
K3.5	724	< .01	191	145	42,526	382	< .01	995	231	20,585	< .01	79

CS: Corn stover (as received)

2.2 Experimental Setup

The microwave experimental schematic of this study is shown in *Figure 2.1*. In this setup, helium gas flows through a capillary valve which allows for precision control of the gas flow from the gas cylinder. The helium gas flow is monitored with a flowmeter, and is then transported to the bottom of the quartz reactor inside of the microwave cavity. Silicone tubing was used because of its microwave transparent characteristics, as well as its high temperature tolerance (for its contact with the hot quartz reactor (*Figure 2.3*), as well as for tolerating the hot exhaust gases). The helium then carries the pyrolysis gases from the heating biomass sample in the quartz crucible out the reactor's top to the exhaust silicone tubing. Three consecutive condensing units containing dichloromethane were placed in ice baths to remove moisture, tar and condensable gases from the exhaust gas stream. Three condensing units were found to be necessary for condensing all condensable products. Non-condensable gases travel to the water-filled graduated gas sampling bulb (1000 mL), which displaces water until the system is at atmospheric pressure. The volume of the non-condensable gases is recorded, and a 250 μ L gas sampling syringe (VICI series-A) was used to extract samples of the gas for gas chromatography characterization. Gases were not collected in the gas sampling bulb for the entirety of the experiment to minimize the helium entering the gas sampling bulb. Instead, the exhaust gas was released into the room until appreciable steam was observed in the first condenser. After this was observed, the exhaust valve was turned to direct emitted gas into the gas sampling bulb for collection. During the gas release period, there was a long, small diameter tube attached to the exhaust valve's outlet to minimize outside air diffusing into the system.

For the CP experiments, the same setup was used, except for the reactor orientation, and the heating element, as shown in *Figure 2.2*. Instead of a microwave cavity, an electric furnace (Lindberg tube furnace, 1400 °C maximum) was used for system heating. Inside of the horizontal electric tube furnace, an alumina tube (914 mm in length x 45 mm i.d.) was used as the reactor, compared to the microwave setup's vertical quartz reactor (200 mm in length x 40 mm i.d.). The reactor orientation and length was assumed to have negligible impact on the results of the pyrolysis experiments, as the flowrate was adjusted to maintain the same gas residence time inside of the reactor.

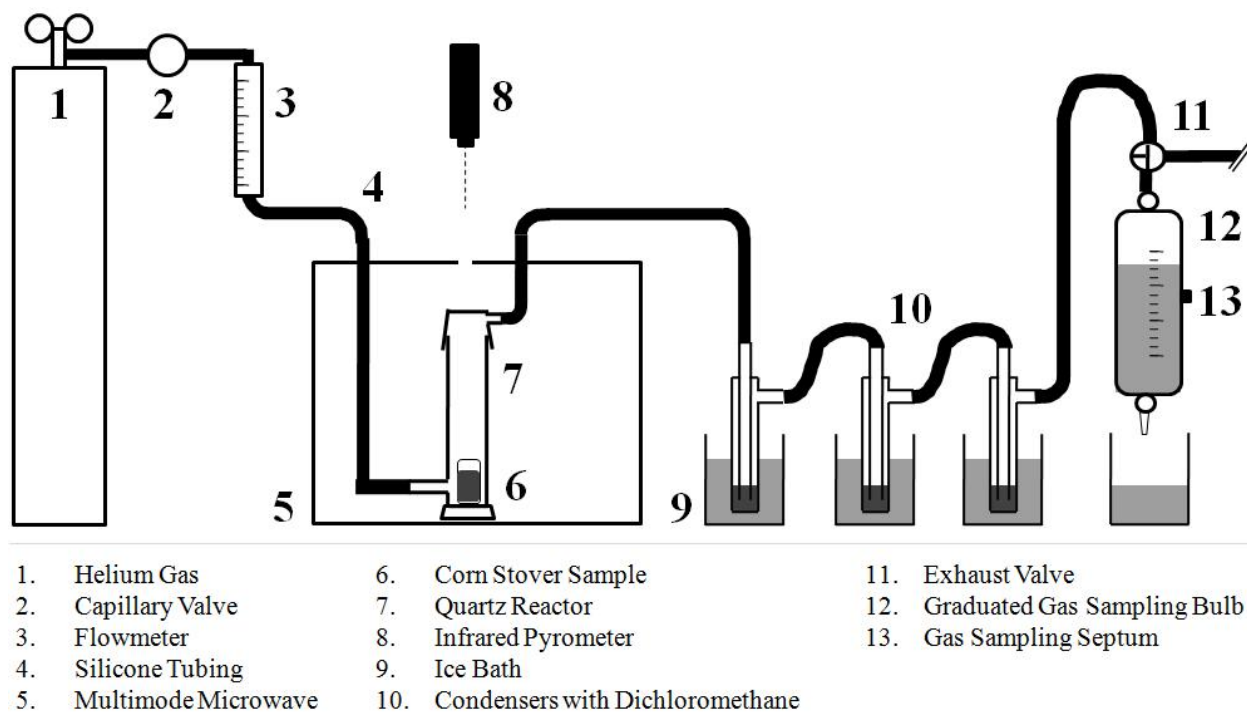


Figure 2.1: Schematic of microwave experiments

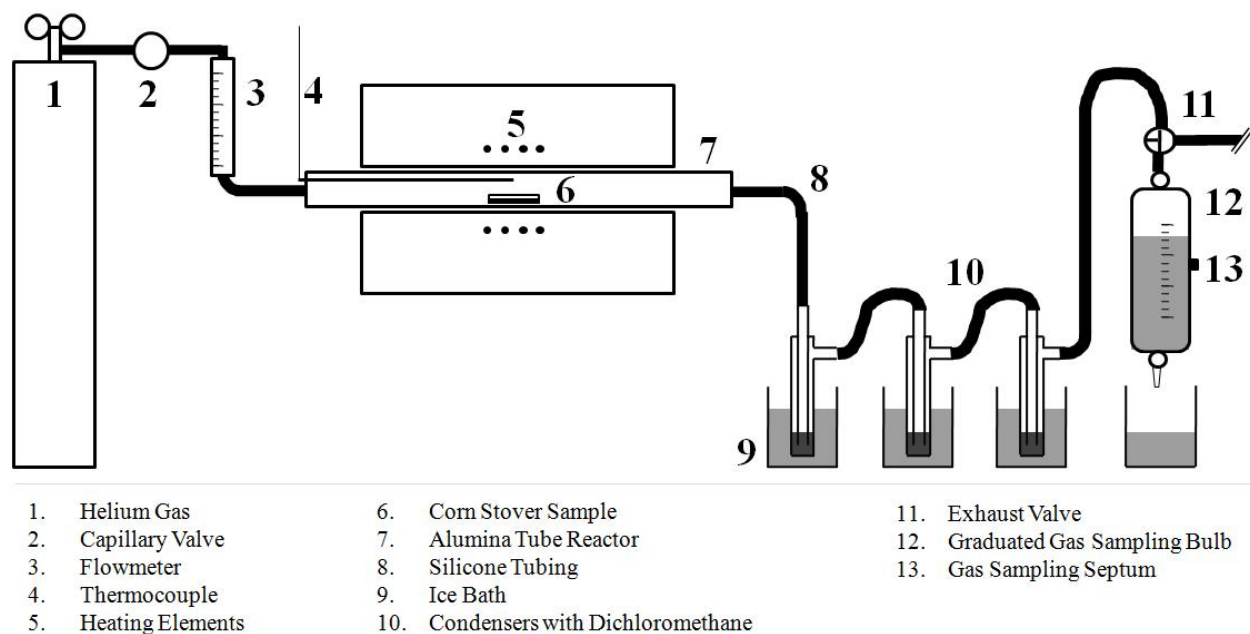


Figure 2.2: Schematic of electric furnace experiments



Figure 2.3: Picture of the quartz reactor used in all MWP experiments. The top and bottom parts of the reactor create an air tight seal through a ground quartz interface

2.2.1 Pyrolysis Conditions

Each of the samples underwent microwave experiments at both 700 and 1000 °C. Only K3.5 was studied in depth at other MWP temperatures. K3.5 was exposed to MWP temperatures of 700, 800, 900 and 1000, and 1100 °C in order to find potassium's optimal temperature. For comparison purposes, CP was carried out at 700 °C for all samples. All experiments carried out at both 700 and 1000 °C underwent duplicate runs to determine experimental repeatability. A temperature variation study was not carried out for CP because potassium catalysis in conventional heating has been well documented. A pyrolysis temperature of 700 °C was chosen for CP experiments because it proved to be the best temperature for potassium's effect in MWP.

In the microwave experiments, a quartz crucible was filled with a homogeneous blend of 0.75 g of corn stover and about 0.075 g of S char from preliminary experiments (microwave receptor), and then inserted into a quartz reactor (4cm x 25cm). The reactor was placed in the center of the

microwave chamber on a sheet of fiberfrax to protect the microwave cavity from the reactor's high temperature. Prior to all microwave experiments, the system was purged with He gas at a flowrate of 500 mL/min, for 45 minutes to minimize oxygen in the quartz reactor. This purging method was found to provide an environment with 0.8 percent (mol.) oxygen. Once the experiment commenced, the gas was exhausted into the room until steam was visible through the condensers, and then the gas was directed to the graduated gas sampling bulb. In all experiments, samples were exposed to microwaves for 5 minutes, and gases were collected for 2 minutes after microwave irradiation (when condenser bubbling slowed substantially) to ensure thorough collection of the product gas in the gas sampling bulb.

In the electric furnace experiments, an alumina reactor (5cm x 90cm) was used. The reactor was purged with He gas at a flowrate of 750 mL/min for one hour to minimize oxygen in the furnace atmosphere. This purging method provided an environment with 1.4 percent (mol.) oxygen. An alumina boat was loaded with about 0.75 g of sample and was placed on the downstream end of the reactor tube, where temperatures were measured to be 200 °C. At this temperature, only an insignificant amount of lignin is known to decompose. The system was then purged further with the end cap sealed for 3 minutes. The gas flowrate was turned down to 400 mL/min (providing the same gas residence time inside both CP and MWP reactors), and the exhaust tube was disconnected to allow a rod to push the sample into the 700 °C zone of the furnace. The exhaust tube was immediately connected. All electric furnace runs exposed samples to 700 °C for 15 minutes, and gases continued to be collected for 2 minutes after sample was moved to the end of the tube (when condenser bubbling slowed substantially.) Samples were allowed to cool for five minutes at the side of the furnace before being removed.

2.2.2 Pyrolysis Temperature

Typically, high temperature processes are monitored through direct-contact measurement devices, such as thermocouples. Microwave heating processes complicate temperature monitoring due to the interference between the emitted electromagnetic waves and the direct-contact monitoring devices [39]. The metal of a thermocouple could respond to the microwave energy, and thus throw off the temperature readings. For this reason, non-contact methods are ideal for monitoring temperatures within a microwave cavity, such as an infrared or an optical pyrometer. In this study, an infrared pyrometer was used to produce a qualitative temperature vs.

time profile during MWP. Infrared pyrometers require a parameter known as emissivity to be the input that describes the monitored surface's ability to reflect radiation. In all electric furnace tests, a thermocouple was used to measure the internal furnace temperature during pyrolysis.

2.2.3 Calibrating Sample's Emissivity

The meaning of emissivity in terms of the infrared pyrometer is the ratio of radiation emitted by the monitored surface to the radiation emitted by a blackbody at the same temperature. A blackbody's emissivity is equal to one, and a highly reflective object would be closer to zero. Since the infrared pyrometer's accuracy is only as good as its entered emissivity, preliminary tests were required to both calibrate the corn stover's emissivity during pyrolysis. Calibrating a rough emissivity value was possible by carrying out several pyrolysis runs with a shard of pyrex in the sample mix. Pyrex was chosen because it does not significantly couple with microwave energy until it reaches melting temperatures, and further it has a known softening point of 820 °C. The idea was to induce pyrolysis at the pyrex's softening temperature, and during the experiment, adjust the pyrometer's emissivity so that the sample temperature was reading just above 820 °C. This method returned an emissivity value of 0.51 for charring corn stover. It is known that emissivity does vary significantly with sample temperature, so it was important to calculate emissivity values for temperatures 700, 800, 900, 1000 and 1100 °C, as these are the various pyrolysis temperatures used in this study. *Figure 2.4* shows the relationship of emissivity plotted against temperature for several carbon based materials. This plot demonstrates how emissivity values were calculated for the case of the corn stover. The trend provided by the numerous points available for graphite provided the corn stover's plot shape, and the emissivity for the corn stover char at 850 °C showed how this trend had to be adjusted to fit the case of corn stover char. *Table 2.3* provides the emissivity values used in the various microwave experiments.

2.2.4 Relating Microwave Power with Pyrolysis Temperature

Creating a relationship between microwave input power and sample temperature is important to this catalytic study because power is the only controllable parameter on the laboratory microwave. Establishing this relationship also started with the preliminary pyrolysis runs with a

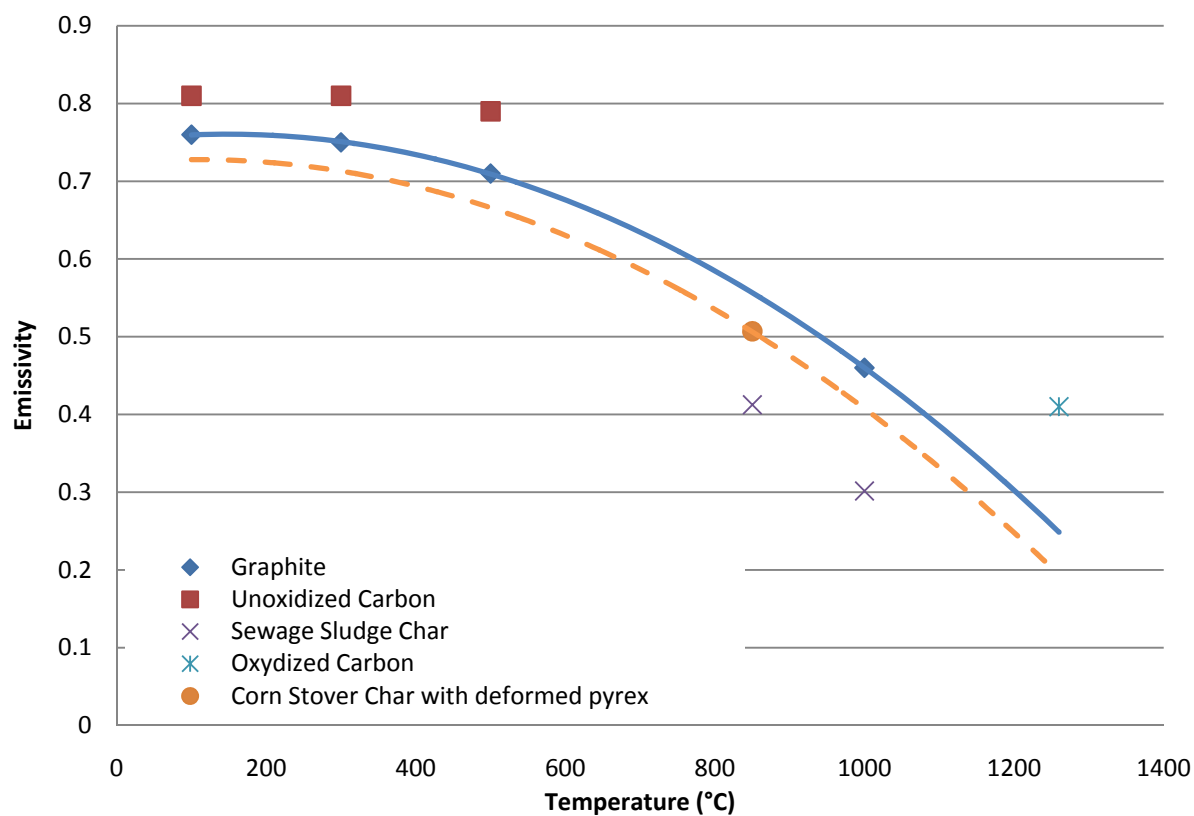


Figure 2.4: Relationship between emissivity and sample temperature for various carbon based materials

Table 2.3: Parameters to reach appropriate MWP temperatures

Feedstock	$T_{\text{pyrolysis}}$ (Celcius)	P_o (W)	P_{final} (W)	Emissivity	$^{\circ}\text{C}/\text{min}$
S	700	1200	650	0.58	438
K0.7	700	1200	650	0.58	337
K3.5	700	800	800	0.58	355
S	1000	1600	1000	0.41	622
K0.7	1000	1600	1000	0.41	455
K3.5	1000	1100	1100	0.41	278
K3.5	800	1000	1000	0.53	251
K3.5	900	1050	1050	0.48	275
K3.5	1100	1150	1150	0.33	-

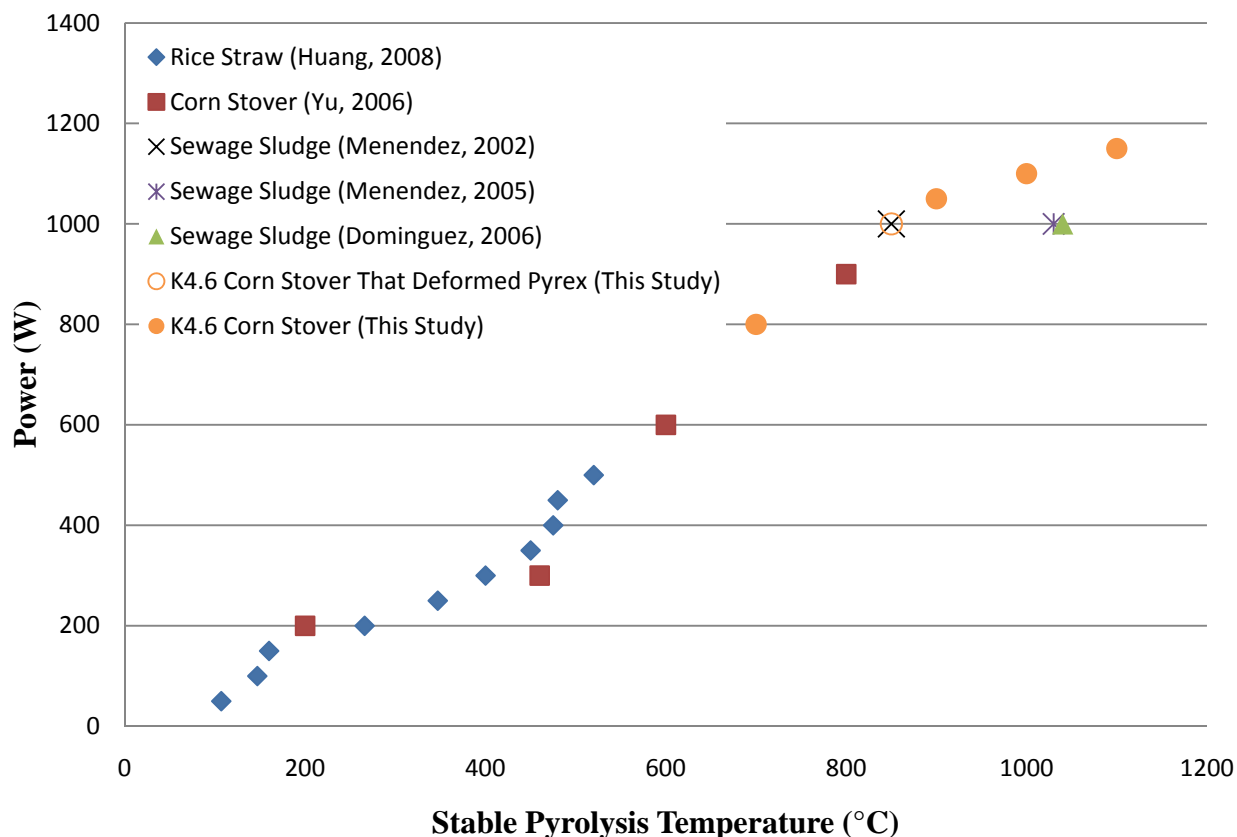


Figure 2.5: Relationship of microwave input power versus pyrolysis temperature

shard of pyrex mixed in with the sample, as pyrex's softening point is known to be 820 °C. The goal was to find the microwave power requirement that allows the corn stover to reach over 820 °C in order to noticeably deform the piece of pyrex. This power requirement was found to be 1000 W, and judging by the subtle melting of the pyrex edges, the temperature reached was approximately 850 °C, which matches up well with other MWP of corn stover studies. *Figure 2.5* demonstrates the relationship of microwave power and pyrolysis temperature of several different microwave-induced pyrolysis of biomass studies. The power values used in this work were derived through trial and error, and they match very well with other corn stover and rice husk studies.

It was difficult for S and K0.7 feedstocks to couple with the estimated power required to reach a given steady pyrolysis temperature. This was difficult because the relationship between power

and temperature was derived with feedstocks with a significant amount of ash content (see *Figure 2.5*), which helped the samples couple with the microwave energy at moderate microwave powers. It is apparent that S and K0.7 did not contain enough ash content to couple similarly to these other natural feedstocks. It was then necessary to start the microwave processing of S and K0.7 at substantially higher powers to get to the desired stable temperature, and once that temperature was reached, the power was reduced accordingly. *Table 2.3* shows the power requirements for each microwave experiment.

2.2.5 Temperature Profiles

Temperature profiles were developed for all but one MWP experiment, as shown in *Figures 2.6* through *2.8*. It can be observed from these plots that microwave heating can achieve repeatable temperature profiles. In *Figure 2.6*, notice that all the plots have fluctuations once the sample reached 700 °C. These fluctuations are due to manually adjusting the microwave power to maintain a consistent pyrolysis temperature. In *Figure 2.7* these fluctuations are not present as much because the power did not have to be reduced as drastically for the 1000 W cases of S and K0.7. *Figure 2.8* shows that in each microwave experiment with K3.5, the power did not have to be adjusted throughout pyrolysis, and that is why there are no abrupt changes in its curves. In some of these figures, drastic fluctuations in temperature can be observed. These are either due to hot spots being picked up by the pyrometer (abrupt temperature rise), or the reactor moving slightly during pyrolysis, so the pyrometer is shortly measuring the temperature of the reactor, which reflects very little radiation back at the pyrometer (abrupt temperature drop). When a temperature drop was observed, the pyrometer was manually held for the duration of the experiment to ensure the sample's temperature profile would be recorded. In only one experiment was there so much reactor movement during pyrolysis (due to tubing rotation) that the pyrometer could not view the sample (experiment K3.5 at 1100 °C), however, the stable temperature was verified at 1100 °C before the sample moved out of view.

Table 2.3 shows the heating rates of these experiments, demonstrating that in the S and K0.7 cases, heating rates are considerably larger than K3.5 due to their larger initial power requirement. These heating rate differences were unavoidable in the microwave experiments and could have an impact on gas production. A previous study verified that heating rates have negligible effect on pyrolysis outcome for stable pyrolysis temperatures greater than 650 °C [52],

which is the case for all of experiments carried out in this thesis. Temperature monitoring of the samples in the electric furnace experiments was not carried out due to the level of difficulty to maintain an air tight system with a thermocouple entering the reactor tube. It was assumed that because the sample was immediately exposed to the 700 °C furnace, a heating rate of at least 350 °C/min was achieved, which is comparable to heating rates achieved through the microwave experiments.

2.3 Methods for Product Analysis

2.3.1 Product Fractions

Sample masses were recorded before and after pyrolysis experiments in order to know the total amount of weight loss during pyrolysis, as well as the resulting char fraction's weight. Char was then placed in an air tight sample container inside of a desiccator.

Condensable volatiles (bio-oil) dissolved in the dichloromethane (DCM) condensers were weighed by measuring the weight of an empty beaker. All DCM from each condenser was then added to the beaker, and placed on a hot plate at 40 °C to slowly evaporate the DCM. After all the DCM was evaporated, bio-oil was the only thing remaining in the beaker. The beaker was then weighed to get the weight of the produced bio-oil that escaped the reactor. In the microwave experiments, there was significant visible bio-oil that had condensed on the reactor walls during each experiment. The reactor weight was therefore measured before and after experiments to get the weight of this condensed bio-oil. Condensation on the reactor walls was not witnessed in any of the electric furnace experiments.

The weight of the gas fraction was calculated by taking the total weight reduction of the sample and subtracting it with the total weight of the bio-oil fraction. This calculation requires the assumption that all moisture from the sample was converted into gas, which is a good assumption considering there was no aqueous fraction observed in the condensing units. The volume of the total product gas was measured to allow for a gas volume production comparison. This was done through the displacement of water in the graduated gas-sampling bulb.

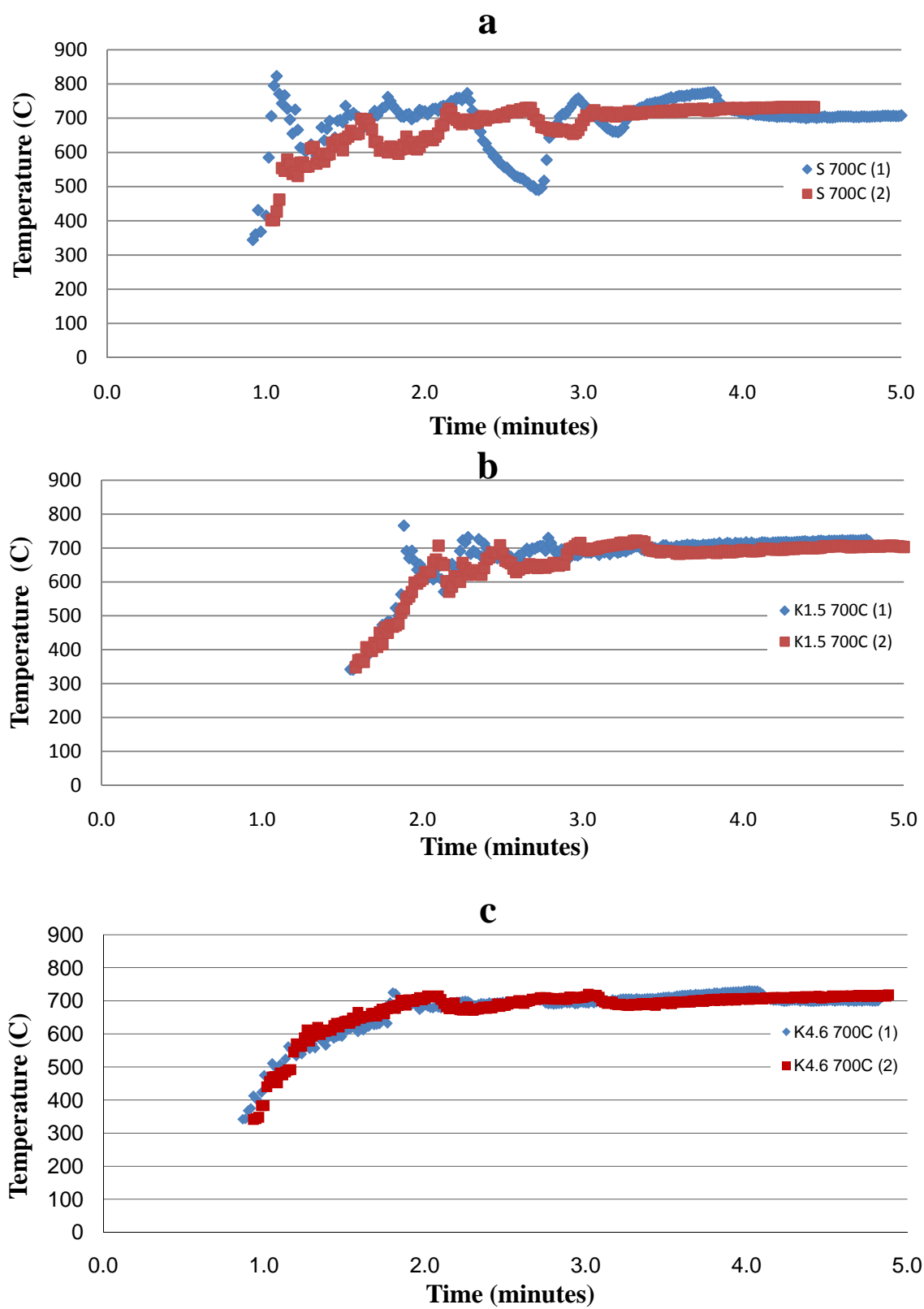


Figure 2.6: Temperature profiles for MWP at 700 °C. a) S; b) K0.7; c) K3.5

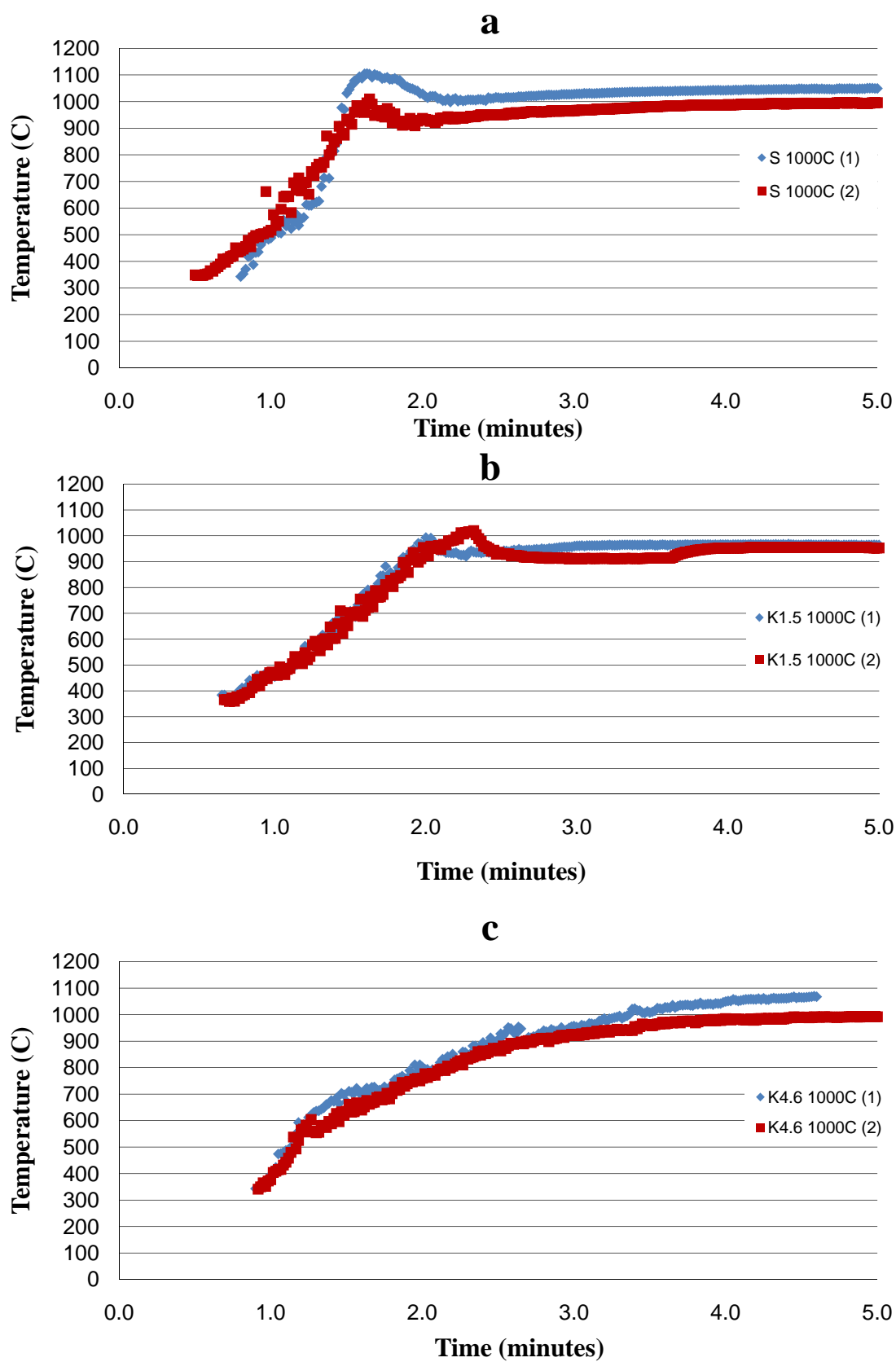


Figure 2.7: Temperature profiles for MWP at 1000 °C. a) S; b) K0.7; c) K3.5

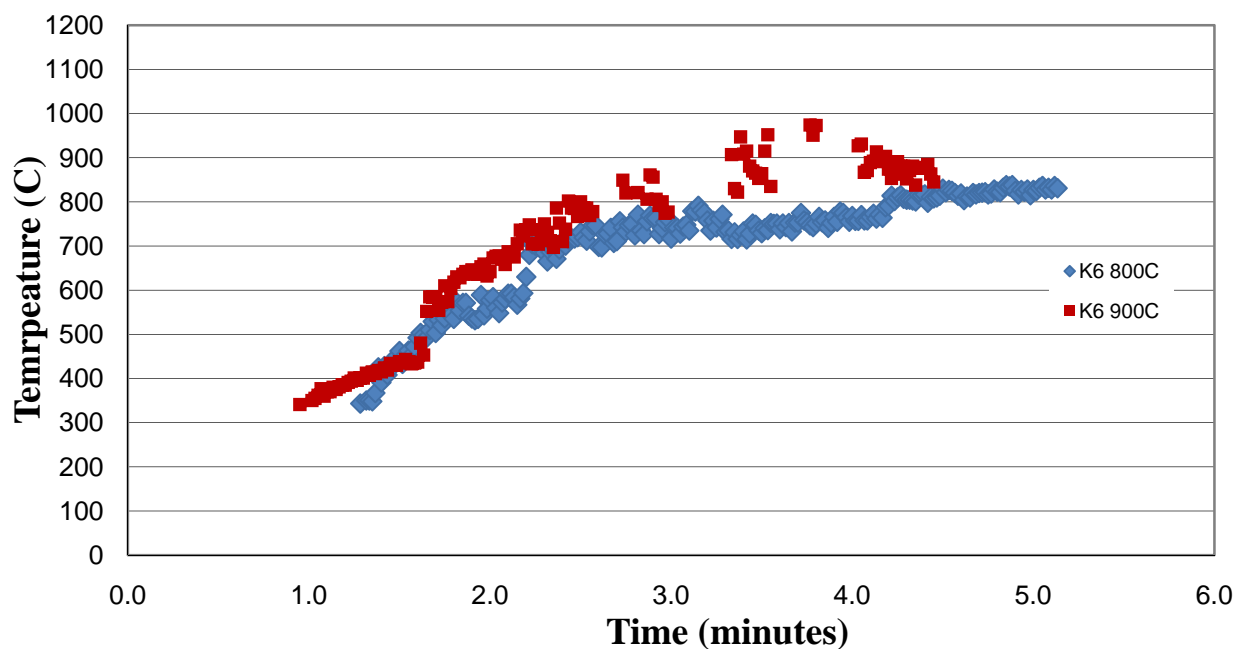


Figure 2.8: Temperature profiles of MWP carried out at 800 and 900 °C for K3.5

2.3.2 Char Methods

The proximate analysis of char was carried out using a Perkin Elmer TGA 7 thermogravimetric analyzer. The ultimate analysis of the char was determined using a LECO TruSpec CHN analyzer, and a LECO SC-144DR sulfur analyzer.

2.3.3 Bio-oil Methods

Bio-oil produced in this work's experiments were not in large enough quantities to meet the requirements for ultimate analysis instruments. The elemental makeup of the bio-oil produced in this work was therefore assumed to be similar to that of oil mallee biomass from a previously done study in order to carry out a final elemental mass balance [14]. Oil Mallee bio-oil makeup was chosen because the feedstock's initial hydrogen and carbon makeup are the closest match to corn stover, from the literature presented in this thesis (see *Table 1.1*.) Oil Mallee's bio-oil properties can be observed in *Table 1.3*.

2.3.4 Bio-gas Methods

All bio-gas produced in this work were characterized utilizing a Shimadzu GC-17A gas chromatograph. Biogas samples of 150 uL were injected for analysis. This gas chromatograph contained two detectors: a thermal conductivity detector (TCD) and flame ionization detector (FID). Both detectors flow He gas at a rate of 20 mL/min. The oven was held at 35 °C for 5 minutes, and then it was ramped at 10 °C/min until 200 °C was reached. The oven temperature was then held at 200 °C for 2 minutes, after which analysis was concluded. Gas standards analysis was done each day of instrument operation to ensure accurate gas quantification.

Chapter 3

EXPERIMENTAL RESULTS AND DISCUSSION

3.1 Product Fractions

Table 3.1 shows the percent weight distribution (ash free basis) of the three possible product fractions: char (solid residue), oil (condensable volatiles), and gas (incondensable-volatiles) for each experiment.

The largest amount of char was produced in the K3.5 CP experiment, which produced 21.3 % char. This experiment yielded the largest char yield because all CP char had trapped volatile matter due to physical restrictions (corn stover particle size), compared to MWP, which heats from the inside of the particle outward, causing volatile matter to build up pressure and essentially force itself out of the particle. With the CP experiments, K3.5 demonstrated the largest char yield because increased potassium loading produced an increase in char yield for both conventional and MWP. Therefore, an increase in potassium loading causes a decrease in devolatilization during pyrolysis, supporting the findings of Morgan *et. al.* [53].

Oil was produced in the greatest amount in the S MWP experiment at 700 °C, which produced 18.7 % oil. MWP produced substantially more bio-oil (at least 4 times more) compared to CP because in MWP, bio-oil condenses in significant amounts on the top reactor walls. This behavior is because during MWP, the reactor walls and gases furthest away from the sample are at significantly lower temperatures than the sample itself, because the sample is the only source of heat; neither gases nor quartz reactor couple with microwaves. This temperature drop coupled with long gas-residence time causes condensation of oil on the reactor walls. Once condensed, the oil might couple with the microwaves for a time, but not enough to escape the reactor. This was not true in the case of CP. The tube of the electric furnace contained no observable oil residue. The most likely reason for this is that the tube and the gases itself downstream of the sample are substantially hotter than in the case of the microwave. These heavy hydrocarbons were likely to have been released initially in similar proportions to that found in microwave

heating; however, these molecules were subjected to high temperatures for a longer period of time leading to significantly more secondary cracking reactions inside the tube furnace. The S case was the largest oil producer of all the feedstocks in MWP because potassium was shown to promote heavy hydrocarbon cracking reactions in MWP.

The best case for gas production was in the S CP experiment which produced 84.7 % gas. CP consistently produced larger gas fractions than MWP at 700 °C. This is mainly due to the difference in oil production between the two heating methods. CP cracks 4 times more heavy hydrocarbons before they leave the reactor compared to MWP.

3.1.1 Effect of Heating Method

Figure 3.1 demonstrates that the most pronounced difference in product fractions when comparing CP and MWP is that MWP produces at least four times more oil. MWP produces substantially more bio-oil (at least 4 times more) compared to CP because in MWP, bio-oil condenses in significant amounts on the top reactor walls. This behavior is because during MWP, the reactor walls and gases furthest away from the sample are at significantly lower temperatures than the sample itself, because the sample is the only source of heat; neither gases nor quartz reactor couple with microwaves. This temperature drop coupled with long gas-residence time causes condensation of oil on the reactor walls. Once condensed, the oil might couple with the microwaves for a time, but not enough to escape the reactor. This was not true in the case of CP. The tube of the electric furnace contained no observable oil residue. The most likely reason for this is that the tube and the gases itself downstream of the sample are substantially hotter than in the case of the microwave. These heavy hydrocarbons were likely to have been released initially in similar proportions to that found in microwave heating; however, these molecules were subjected to high temperatures for a longer period of time leading to significantly more secondary cracking reactions inside the tube furnace. This in turn gave CP a larger gas fraction yield compared to MWP. An increase of 3.5 percent in potassium caused MWP's gas fraction to remain fairly constant; whereas in CP, this potassium addition decreased the gas fraction by 9 percent.

Another less significant explanation for the discrepancy in oil production between the two heating methods is that during the drying stage in MWP moisture escapes violently from inside

Table 3.1: Product Fraction Results (in weight % on ash free basis)

	CP			MWP								
	700 °C			700 °C			1000 °C			800 °C	900 °C	1100 °C
	S	K0.7	K3.5	S	K0.7	K3.5	S	K0.7	K3.5	K3.5	K3.5	K3.5
Char	12.9 ± 0.4	20.1 ± 0.1	21.3 ± 2.8	10.5 ± 0.2	15.2 ± 0.2	15.6	6.8 ± 0.0	11.3 ± 0.2	13.6 ± 0.5	15.9	15.2	12.7
Oil	2.4 ± 0.2	3.5 ± 0.3	3.0 ± 0.2	18.7 ± 5.6	17.4 ± 1.4	12.9	8.7 ± 0.8	7.2 ± 1.8	6.2 ± 2.8	10.0	4.7	4.2
Gas	84.7 ± 0.2	76.4 ± 0.4	75.7 ± 2.6	70.8 ± 5.4	67.4 ± 1.2	71.6	84.5 ± 0.9	81.5 ± 1.9	80.1 ± 3.3	74.0	80.1	83.1

of the biomass, causing an elaborate pore structure network as demonstrated by Wang *et. al.* This pore network then creates an easy passage for volatiles being released later during pyrolysis to escape with a shorter particle residence time. This shorter particle residence time inhibit secondary cracking reactions that would break down heavy hydrocarbons into simpler, incondensable gases [32]. The result from this elaborate pore structure created during microwave drying is a slightly larger oil fraction compared to CP. This trend is also verified further in the *Analysis of Gas* section. For MWP, adding 3.5 percent potassium decreased oil yield 5.8 percent; whereas for CP, this potassium addition increased oil yield a marginal 0.6 percent.

CP was shown to produce slightly more char than in MWP. Volatile matter was later found in the char of each CP run, which led to the conclusion that the samples met physical restrictions (corn stover particle size), and that this difference could have been avoided with a finer particle size. In MWP and CP, adding 3.5 percent potassium increased char yields 5.1 and 8.4 percent, respectively.

3.1.2 Effect of Potassium Loading

It has been well demonstrated that addition of catalyst metals inhibits devolatilization during pyrolysis [15, 53-57]. This behavior is also verified in this study in *Figure 3.1*. It is for this reason that the char fraction (ash free basis) increases with potassium loading for both heating methods and at different temperatures. A potassium loading of 0.7 percent was enough to increase char by at least 4.5 percent of ash free sample weight. Increased potassium loading had a relatively insignificant effect on char, except for pyrolysis occurring at 1000 °C which increased 2.3 percent of ash free sample weight between K0.7 and K3.5.

In the case of the oil fraction, MWP demonstrated a decreasing trend of oil with increased potassium loading. At 700 °C, there was a slight decrease between S and K0.7 feedstocks, but a significant drop in oil production between K0.7 and K3.5 feedstocks. This shows that for MWP at lower temperatures, a potassium loading between 0.7 and 3.5 percent promotes secondary cracking reactions of heavy hydrocarbons. The total decrease in the oil fraction from 3.5 percent potassium loading is 5.8 percent. At 1000 °C, there was a linear decrease of oil production with potassium loading, yielding a total decrease of 2.5 percent. The reason for this discrepancy

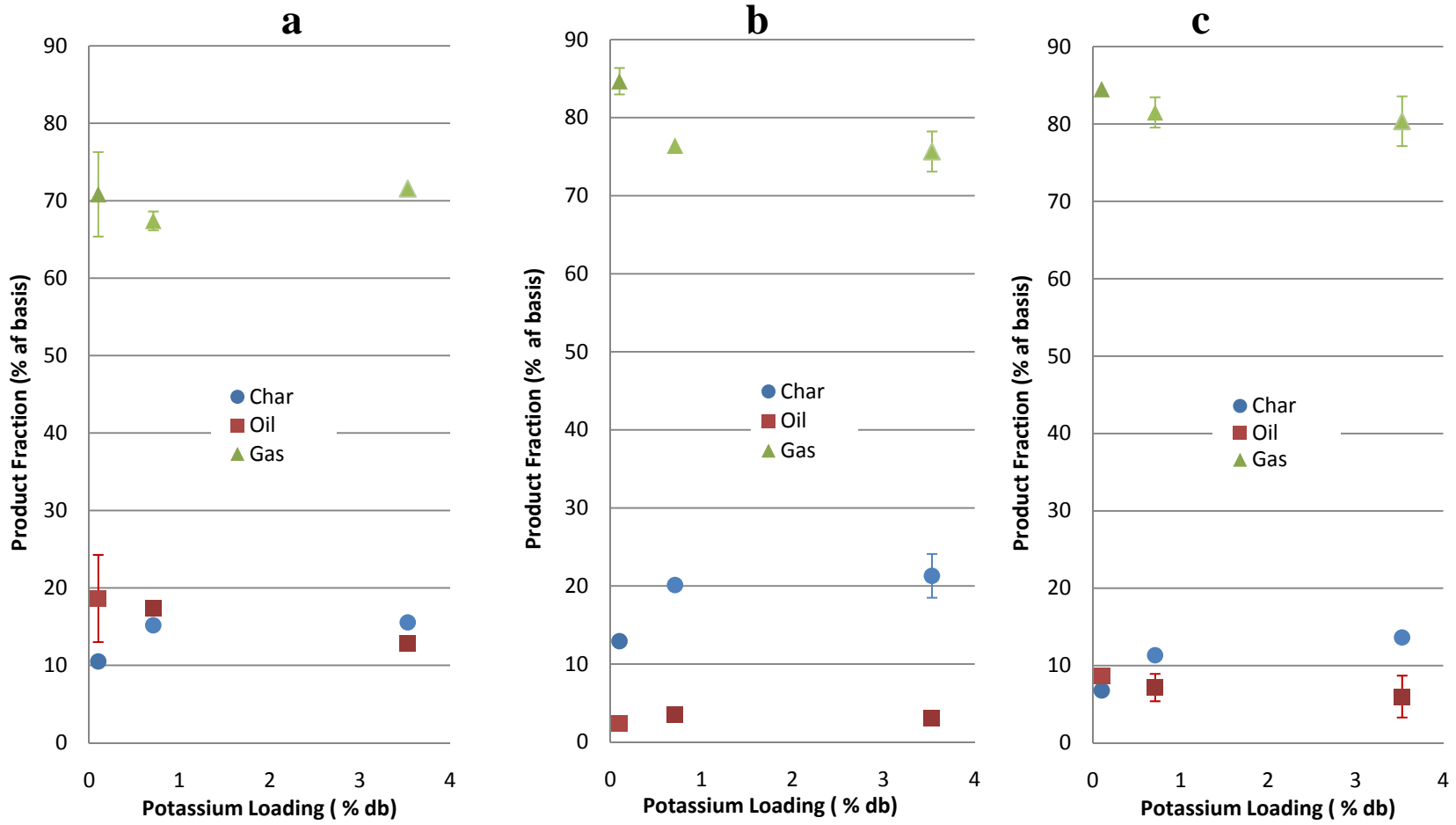


Figure 3.1: Product fractions versus potassium loading. a) CP at 700 °C; b) MWP at 700 °C; and c) MWP at 1000 °C

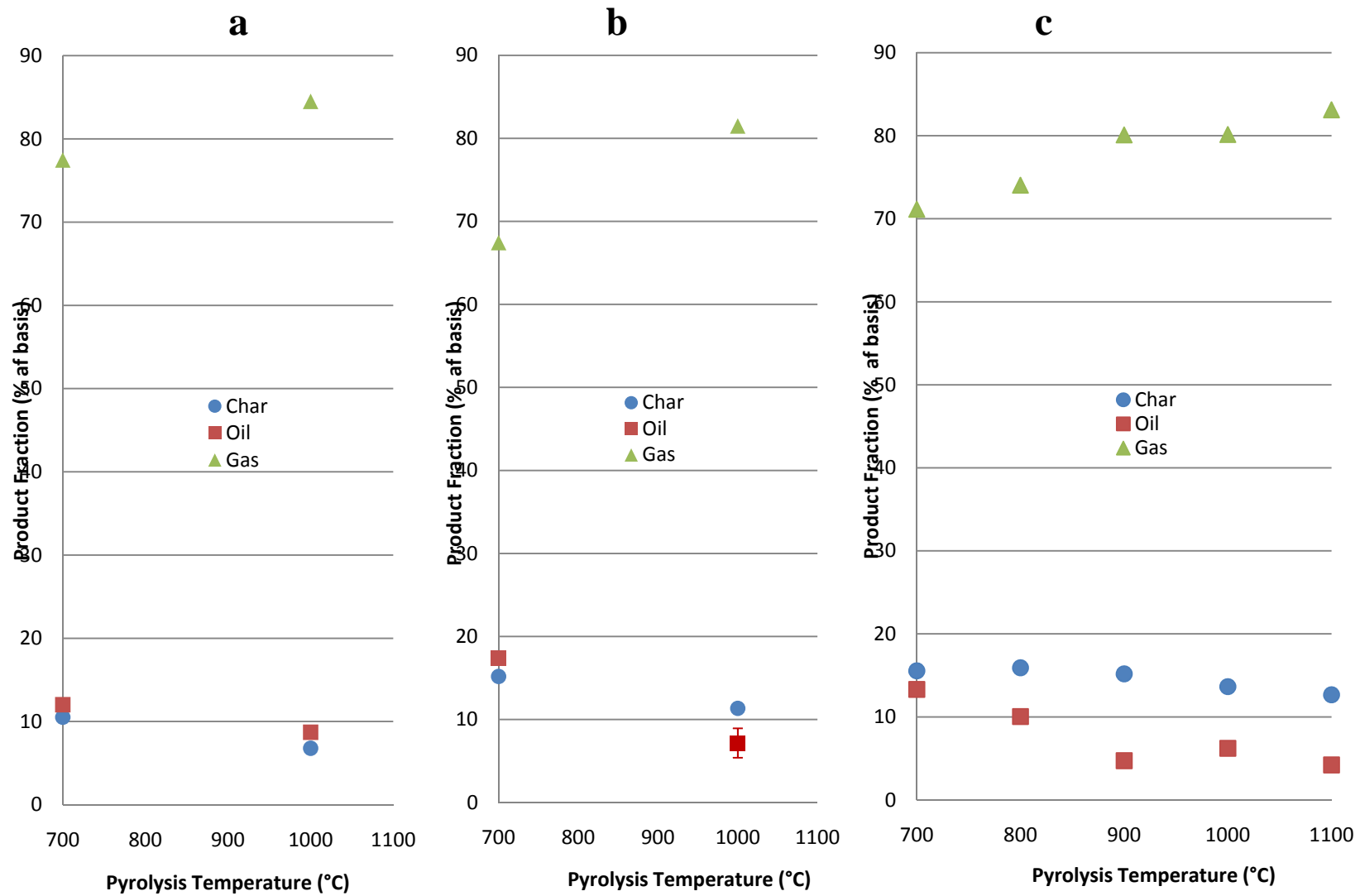


Figure 3.2: Product fractions versus temperature. a) is for S; b) is for K0.7; and c) is for K3.5

between pyrolysis behaviors is that when comparing bio-oil productions for feedstock S, the bio-oil fractions for 700 and 1000 °C are 18.7 and 8.7 percent, respectively. This shows us that higher pyrolysis temperatures produce less than half the quantity of bio-oil, thus halving the secondary cracking reactions promoted by potassium addition. Potassium loading in general decreases the gas fraction in each type of experiment because potassium's pyrolysis inhibiting behavior is more significant than its promoting of secondary cracking reactions. In other words, char is increased with potassium loading at a greater rate than oil's decrease with potassium loading. In the case of MWP of 700 °C however, the gas fraction was found to be about the same regardless of potassium loading because the char increase and oil decrease were very similar, thus offsetting each other when calculating the gas fraction by difference. At 1000 °C, a potassium loading of 3.5 percent caused a decrease in the gas fraction of 4.4 percent.

3.1.3 Effect of Temperature

Temperature increase has been demonstrated to increase the gas fractions at the expense of the oil and char fractions [34]. This behavior is also found in *Figure 3.2* for all feedstocks, but it also shows that in the case of K3.5, between 700 and 900°C, char fractions remain relatively constant. Beyond 900 °C though, char is shown to decrease proportionately with pyrolysis temperature (-1.25 percent per 100 °C). Higher temperatures have been demonstrated to promote heterogeneous reactions, providing an explanation for this behavior [37].

When observing oil production behavior versus temperature, it is apparent from *Figure 3.2c* that there is large decrease in oil production between 700 and 900 °C (-4.1 percent per 100 °C), beyond which, the production remains constant. This behavior shows that up to 900 °C, secondary cracking reactions of heavy hydrocarbons are increasing, and beyond 900 °C, bio-oil is escaping the reactor too rapidly to be cracked. This behavior may be true in the cases of S and K0.7, but this was not verified in this study.

Figure 3.2c also reveals that the gas fraction increases drastically between 700 and 900 °C (4.25 percent per 100°C), and moderately beyond 900 °C (0.7 percent per 100 °C). The drastic increase can be attributed to heavy hydrocarbon cracking and the moderate increase from the promotion of heterogeneous reactions.

3.2 Analysis of Char

The proximate and elemental analysis of the char produced from each experiment can be found in *Table 3.2*. The first thing to notice in this table is that the volatile matter in all K3.5 char is much higher than anticipated (explained further in *Effect of Potassium* section), however, S and K0.7 chars' volatile content are for the most part similar to other biomass derived pyrolytic char presented in *Table 1.4*. Both hydrogen and oxygen were found in the char for each CP run. This phenomenon was due to the corn stover's fairly large particle size, which left trapped volatile matter in the center of the corn stover particles. Hydrogen was not observed as much in MWP because in MWP, samples are heated from the inside out, causing pressure to build from biomass devolatilization in the center of the particle, so any volatiles trapped physically within the particle end up bursting out of the particle from the built up gas pressure. This is supported further with the fact that runs using less microwave power produced more char with subtle traces of hydrogen and oxygen compared to runs using more microwave power. Increasing microwave power increases the pressure of internally "trapped" volatiles, therefore promoting their release. K3.5 derived char show significant oxygen remaining, alongside a significantly increased char fraction compared to feedstock S. These facts suggest that potassium inhibits the pyrolysis of oxygen containing compounds.

Figure 3.3 shows char's ash and volatile matter as a function of potassium loading. It is evident from these plots that the volatile matter content in K0.7 derived char is low relative to both S and K3.5 derived char under the same conditions. It was also found that the K0.7 corn stover contained the lowest volatile matter content. This means that for an unknown reason, K0.7 corn stover is inhibited to release some of its volatiles, as it went through the same preparation procedures as the other corn stover types.

3.2.1 Effect of Heating Method

When using *Figures 3.3a* and *3.3b* to compare char makeup differences between heating methods, it can be observed that for the most part, these plots look very similar. The significant difference between the two plots is that for K3.5, CP produced a char with an ash percentage far less than in MWP. This difference is because the K3.5 char from CP had the greatest amount of unreleased hydrogen and oxygen of each feedstock type, thus making its ash percentage lower.

Table 3.2: Properties of char produced in each experiment

Sample	T (°C)	HM	Ash ^a	VM ^b	FC ^{b,c}	Organic Fraction ^b				
						C	H	N	S	O ^c
S	700	EF	6.1	14.1	85.9	98.7	0.2	0.7	0.1	0.4
K0.7	700	EF	6.6	11.0	89.0	98.4	0.5	1.0	0.1	-
K3.5	700	EF	2.3	46.9	53.1	84.0	0.5	0.3	0.1	15.2
S	700	MW	19.2	16.6	83.4	99.1	-	0.9	0.1	-
K0.7	700	MW	9.3	10.2	89.8	98.6	-	1.4	0.1	-
K3.5	700	MW	1.6	42.0	58.0	89.8	0.1	0.8	0.1	9.3
S	1000	MW	10.8	36.0	64.0	95.7	-	0.9	0.1	3.3
K0.7	1000	MW	13.0	6.1	93.9	98.9	-	1.0	0.1	-
K3.5	1000	MW	5.0	48.7	51.3	96.7	-	0.5	0.1	2.7
K3.5	800	MW	3.1	46.7	53.3	95.8	0.4	0.9	0.1	2.8
K3.5	900	MW	0.5	41.6	58.4	91.5	-	0.3	0.1	8.1
K3.5	1100	MW	3.3	37.5	62.5	95.5	-	0.7	0.1	3.7

^a Dry, K₂O free basis^b Dry, ash free basis^c Calculated by difference

3.2.2 Effect of Potassium Loading

It can be observed in *Figure 3.3* for all pyrolysis conditions that ash content in char decreases with potassium loading, on a dry, K₂O free basis. There is significant volatile content being observed in every K3.5 char (explaining decreasing ash trend), which necessitates further investigation. TGA-MS analysis was carried out on several chars to explain this behavior. This analysis showed that for S and K0.7 char produced at 700 °C, chloride compounds made up the majority of the char's volatile content, followed by trapped moisture. K3.5 corn stalk samples started out with the most moisture of all the samples, and correspondingly, K3.5 char showed the largest trapped moisture release during the volatile stage of proximate analysis. Volatiles observed from K3.5 mainly consisted of this trapped moisture, and to a lesser extent, chloride compounds. The chlorine existed in each biomass sample from the acid washing sample preparation step. The chlorine made up a substantial amount of the char's weight after volatile weight loss during pyrolysis. For an unknown reason, the chlorine was not released during pyrolysis, but instead during char proximate analysis.

3.2.3 Effect of Temperature

Microwaved pyrolytic char's ash, volatile matter and fixed carbon content are not affected by the pyrolysis temperature for sample K0.7 (see *Figure 3.3.*) In the case of S's microwaved pyrolytic char, volatile matter increased substantially with pyrolysis temperature. Keep in mind that char derived from microwave experiments contain essentially ash, and carbon. In the case of K3.5 derived char, ash percentage remained constant up to 900 °C, and increased beyond this temperature. The percentage of ash in char increases past 900 °C because more heterogeneous reactions are promoted at these higher pyrolysis temperatures, thus removing more carbon from

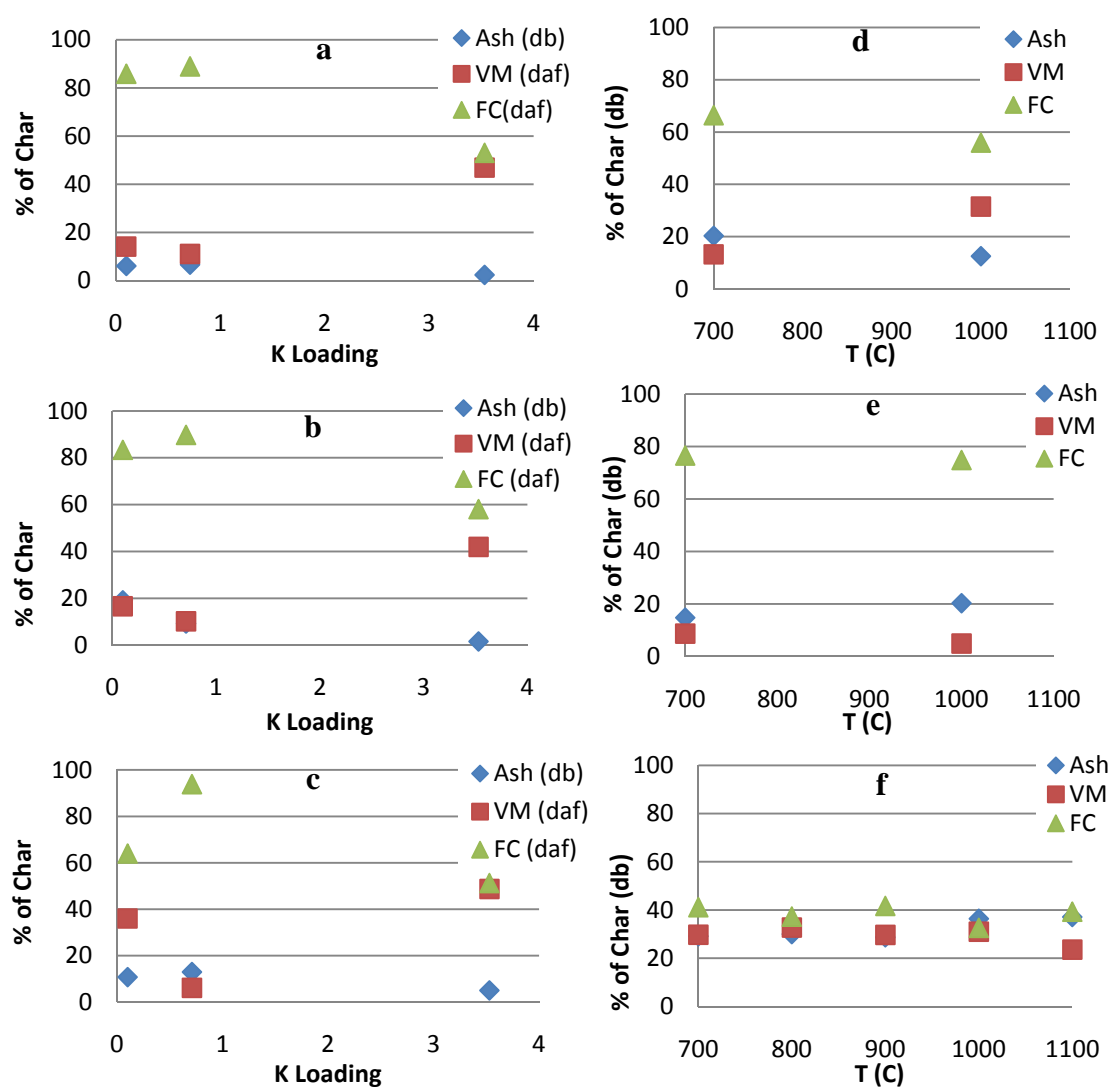


Figure 3.3: Proximate analysis results for char plotted against potassium and temperature. Ash values are displayed on a dry, K₂O free basis. The different plots are: a) CP at 700 C; b) MWP at 700 C; c) MWP at 1000 C; d) S MWP e) K0.7 MWP f) K3.5 MWP

the char. These conclusions are also supported by *Figure 3.2c*, which shows the char fraction decrease past 900 °C.

3.3 Analysis of Gas

The incondensable gases produced from each experiment are presented in *Table 3.3* in two different forms. The top part of the table provides the volume of gas constituent produced per gram (ash free) of corn stover, while the bottom section of the table provides the gas constituent's molar percentage of the total product gas mixture. The molar percentage values provide an easy means to compare stoichiometric relationships between constituents in order to explain specific reactions that are being promoted by specific variables. The highest values for each constituent are printed in bold for convenience.

Volumes of both H₂ and syngas (H₂ + CO) were optimized in the case of MWP of S at 1000 °C. This is because in general, MWP produces substantially larger H₂ volumes compared to CP, and higher pyrolysis temperatures have been demonstrated to increase syngas production [31]. As stated previously, in MWP, increasing temperatures beyond 700 °C increases secondary cracking of heavy hydrocarbons, and past 900 °C, heterogeneous reactions are promoted that convert more carbon into gas. Of all of the feedstocks, S produced the most syngas at 1000 °C because potassium's inhibiting volatile release behavior had a significantly greater effect at high temperature than its heavy hydrocarbon cracking tendency.

The volume of CO₂ produced was maximized in the case of MWP of K3.5 at 900 °C. This behavior is observed because the water-gas shift reaction is favored at this temperature. Also, potassium loading increases this reaction, so K3.5 produced the largest volume of CO₂. Water-gas shift reactions can be considered good if the biogas will be used in a power production facility with carbon capture, as some of the CO is already converted to CO₂, but in the case of Fischer Tropsch synthesis application, this reaction would have a negative effect on the final application.

In the case of non-condensable hydrocarbon production, CP out-produced MWP. This finding agrees with other studies [5, 9]. MWP favors dry reforming of hydrocarbons with CO₂, as well as the methane decomposition. This behavior is not observed on the same scale in CP, most

likely because CP favors the secondary cracking of hydrocarbons, leading to a gas with significant light hydrocarbons. At each experimental condition, CH_4 and C_2H_6 were produced in the largest amounts with both S and K0.7 because when taking into account their respective errors, their values overlap. When comparing S and K0.7's product fractions in each experimental condition, it is clear that oil remains almost constant. This can be interpreted as verification that CH_4 and C_2H_6 production are a direct result from secondary cracking of heavy hydrocarbons.

3.3.1 Effect of Heating Method

Figure 3.4a is a summary of gas analysis data to compare MWP and CP's total gas and syngas productions at 700 °C. It is evident from this plot that potassium loading increases the total gas and syngas volumes of MWP much more than CP. This is because MWP produced substantially higher hydrogen volume in the case of K3.5, and hydrogen's density is orders of magnitude lower than the other product gases. From this it can be concluded that at 700 °C, a potassium loading between 0.7 and 3.5 percent promotes syngas production substantially more for MWP compared to CP. It should also be noted that regardless of potassium loading, MWP produced more syngas than CP. In the case of K3.5, MWP produced 36 ml/g (ash free) more syngas than CP.

Figures 3.5a and *3.5b* can be used to compare how the type of heating method effects the production of pyrolytic gas. The most substantial difference between the two heating method's gas production is the drastically higher amount of hydrogen produced during MWP. Hydrogasification reactions are evident more in MWP than CP, as shown by microwave's substantially smaller char yield. It was concluded that differences in hydrogasification were not due to inherent differences in heating method, but instead due to the experimental procedural differences between the two heating methods. In each electric furnace experiment, samples were preheating when initially placed in the downstream end of the furnace tube. When the system was then left to purge for several minutes to minimize oxygen in the environment, it is likely that significant moisture had been evaporated before pushing the sample into the hot zone of the furnace, thus practically eliminating water vapor from pyrolysis reactions.

Table 3.3: Gas production analysis for all experiments

		CP			MWP								
		700 °C			700 °C			1000 °C			800 °C	900 °C	1100 °C
		S	K0.7	K3.5	S	K0.7	K3.5	S	K0.7	K3.5	K3.5	K3.5	K3.5
Product Gas Volume (ml/g af)	H ₂	17 ± 0.9	14 ± 0.4	30 ± 0.8	47 ± 3.9	43 ± 7.3	73	88 ± 2.5	73 ± 0.4	70 ± 2.7	65	70	85
	CO	90 ± 1.2	81 ± 13.6	81 ± 1.0	69 ± 7.5	66 ± 18.8	74	120 ± 3.1	115 ± 7.4	83 ± 8.4	72	71	104
	CO ₂	7 ± 1.3	6 ± 5.8	17 ± 7.8	6 ± 1.3	7 ± 1.7	9	5 ± 1.3	11 ± 2.5	13 ± 1.6	12	20	16
	CH ₄	22 ± 1.2	24 ± 3.6	16 ± 8.1	11 ± 1.1	11 ± 4.2	7	18 ± 0.4	19 ± 1.3	9 ± 0.8	8	8	10
	C ₂ H ₆	6 ± 1.5	4 ± 1.2	4 ± 2.1	2 ± 0.2	1 ± 0.6	1	3 ± 0.1	3 ± 0.0	3 ± 0.5	2	2	2
	H ₂ +CO	107 ± 2.2	96 ± 14.0	111 ± 1.8	116 ± 11.4	109 ± 26.1	147	208 ± 5.5	188 ± 7.8	153 ± 11.1	137	141	188
	Total	142 ± 6.2	129 ± 24.6	149 ± 19.7	134 ± 14.0	128 ± 32.6	165	234 ± 7.3	221 ± 11.6	178 ± 14.0	158	171	216
Product Gas Composition (mol %)	H ₂	12 ± 0.4	11 ± 1.8	21 ± 2.2	35 ± 0.7	34 ± 3.1	44	38 ± 0.1	33 ± 1.8	40 ± 1.4	41	41	39
	CO	64 ± 2.6	63 ± 1.5	55 ± 6.7	51 ± 0.2	51 ± 1.8	45	51 ± 0.3	52 ± 0.8	47 ± 1.3	46	41	48
	CO ₂	5 ± 0.8	4 ± 3.8	11 ± 3.8	4 ± 0.6	5 ± 0.1	6	2 ± 0.5	5 ± 0.9	7 ± 0.4	8	11	7
	CH ₄	15 ± 0.5	19 ± 0.8	10 ± 4.1	8 ± 0.1	9 ± 1.1	4	8 ± 0.1	9 ± 0.1	5 ± 0.1	5	5	5
	C ₂ H ₆	4 ± 1.0	3 ± 0.4	3 ± 1.1	1 ± 0.0	1 ± 0.3	1	1 ± 0.0	1 ± 0.1	1 ± 0.4	1	1	1
	H ₂ +CO	76 ± 2.9	75 ± 3.4	76 ± 8.9	86 ± 0.5	85 ± 4.9	89	89 ± 0.4	85 ± 2.6	86 ± 2.7	87	82	87
	H ₂ /CO HHV	0.19	0.18	0.37	0.68	0.68	0.99	0.74	0.64	0.85	0.89	0.99	0.82
(MJ/m ³)	17.2	17.7	14.6	14.1	13.8	12.7	14.3	14.3	13.0	12.6	12.4	12.6	

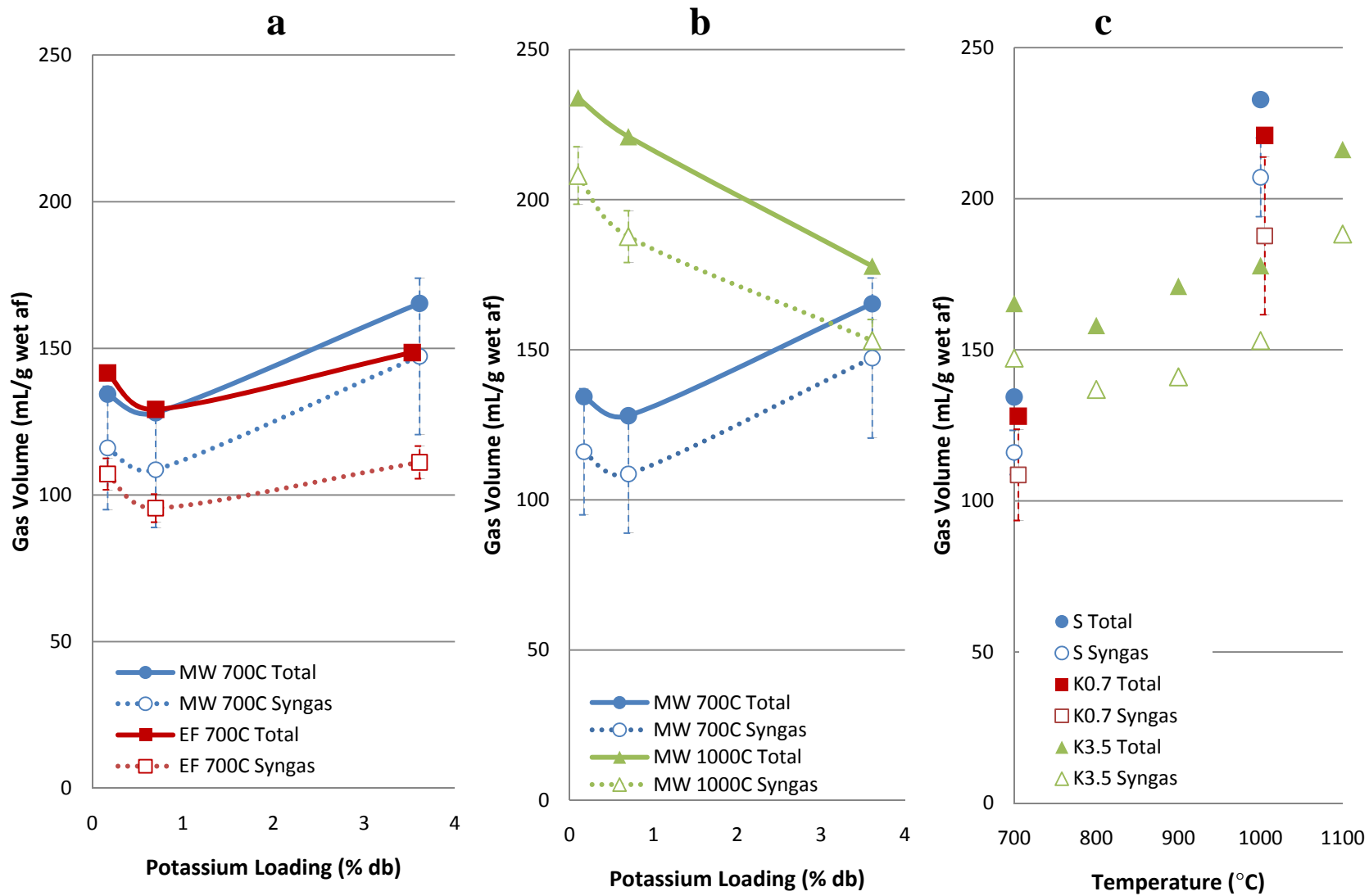


Figure 3.4: Syngas production plotted against both potassium loading and temperature.

It should then be observed that this procedural error will actually help determine the extent of both methane decomposition, as well as hydrogasification taking place in MWP. Because CP had negligible moisture to react during pyrolysis, this creates a comparison for MWP in order to determine the extent of hydrogasification in MWP experiments done at 700 °C. However, it was first required to verify that changes in CH₄ and H₂ with potassium loading make stoichiometric sense with methane decomposition, and any excess H₂ produced in MWP can be assumed to be derived from hydrogasification (see *Table 3.4* for the computation values.) It is evident that in the case of CP, methane decomposition explains the increase of H₂ between K0.7 and K3.5. It is also evident from this table that in MWP, K3.5 had more hydrogasification take place than S and K0.7 did. By averaging the H₂ volumes of S and K0.7 samples for MWP, and subtracting this average with the average of H₂ volumes of S and K0.7 samples for CP, this gives the volume of H₂ produced through hydrogasification in samples S and K0.7. The summary of these volumetric calculations are found in *Table 3.5*. After further calculations were carried out, it was found that volumes of CO produced from hydrogasification correspond to the volumes of H₂.

In the case of CP, it was found that a potassium loading increase from 0.7 to 3.5 percent increased H₂ production by 14.5 mL/g (ash free) through methane decomposition. As for MWP, this same potassium loading increase provided a H₂ production increase of 23mL/g (ash free). This means that microwaves increase potassium's promotion of the methane decomposition reaction by 60.7 percent at 700 °C. This discrepancy could be due to the fact that microwave heating does not heat two different materials to the same temperature. Once it reaches a high enough temperature, potassium becomes a good receptor of microwave energy, causing potassium to achieve higher temperatures than the rest of the sample [39]. This was found to be true in preliminary experiments, where feedstock K3.5 require the least microwave input power for this very reason (see *Table 2.3*.) This anisothermal condition, which was discussed previously, drastically increases reaction rates compared to conventional heating [2]. In this case, potassium's known catalytic effect will be increased due to MWP's tendency to increase reaction rates.

Now, hydrogasification reactions taking place in MWP at 700 °C should be discussed. Feedstocks S and K0.7 produced both H₂ and CO derived from hydrogasification in the amount of 29.5 mL/g (ash free). In the case of sample K3.5, 34.5 mL/g (ash free) of both H₂ and CO

were produced from hydrogasification reactions. The extent of hydrogasification was greater for K3.5 because of its higher moisture content.

CP produced consistently higher CO values (at least 7 ml/g (ash free) higher), which is typically an indicator of more secondary cracking reactions [62]. Another indicator of this is the significantly larger production of light hydrocarbons in the case of CP. This can be explained by microwave drying behavior creating an elaborate pore structure that decreases these secondary reactions, as discussed previously in the *Product Fractions* section.

CO₂ production was not influenced by the heating method, which says that heating method did not alter the reactions involving carboxylic functional groups, the main source of CO₂ in pyrolysis.

Table 3.4: Stoichiometric calculations for pyrolysis reactions

	CH ₄ Production (mol. %)			H ₂ Production (mol. %)			CH ₄ Decomp. (% Δ H ₂)	Hydrogas. (% Δ H ₂)
	avg S, K0.7	K3.5	Δ	avg S, K0.7	K3.5	Δ		
CP	17.0	12.6	-4.5	11.6	20.6	9.0	100.0	0.0
MWP	8.4	4.4	-4.0	34.7	44.4	9.7	82.3	17.7

Table 3.5: Volumetric calculations for pyrolysis reactions

	CH ₄ Production (mL/g (af))			H ₂ Production (mL/g (af))			CH ₄ Decomp. (ml/g (af) H ₂)	Hydrogas. (ml/g S, K0.7 (af) H ₂)	Hydrogas. (ml/g K3.5 (af) H ₂)
	avg S, K0.7	K3.5	Δ	avg S, K0.7	K3.5	Δ			
CP	22.9	16.0	6.9	14.6	30.0	14.5	14.5	0.0	0.0
MWP	11.2	7.0	4.2	45.0	73.0	28.0	23.0	29.5	34.5

3.3.2 Effect of Potassium Loading

The gas production summaries of microwave experiment carried out at 700 and 1000 °C are plotted against potassium loading in *Figure 3.4b*. The most important trend from this plot is that increasing pyrolysis temperature causes syngas to increase significantly for every feedstock. It should also be noted that pyrolysis temperature has significant effect on potassium's influence on

pyrolysis. At 700 °C, potassium loading increase from 0.7 to 3.5 caused syngas production to increase by 38 ml/g (ash free). At 1000 °C, syngas production decreased proportionately with potassium loading at a rate of -10 ml/percent potassium loading, with a total decrease totaling 55 ml/g (ash free). This behavior resulted because at the higher temperature, potassium's pyrolysis inhibiting tendency was more pronounced than its promoting of oil cracking, resulting in a decreasing gas fraction with potassium loading. Potassium's inhibiting effect has been well demonstrated in previous studies [20, 53]. At 700 °C, the inverse of this was true. In essence, temperature determines which of potassium's effects dominate pyrolysis behavior. *Figure 3.4b* demonstrates that the syngas increase caused by potassium loading at low temperatures is overshadowed by the syngas increase from increasing the microwave pyrolysis temperature. The relationship of the production of syngas with potassium loading at 1000 °C is provided below.

$$V_{\text{syngas}} = -10.032K + 207.61$$

Individual gas products produced for microwave pyrolysis temperatures of 700 and 1000 °C are presented in *Figure 3.5*. At 700 °C, a potassium loading increase from 0.7 to 3.5 percent increases H₂ dramatically at the expense of CH₄. *Figure 3.6* provides stoichiometric verification that the decomposition of methane was promoted with potassium levels between 0.7 and 3.5 percent. At 1000 °C, however, potassium addition greater than or equal to 0.7 percent decreases H₂ production by about 15 ml/g (ash free). As stated above, this is because pyrolysis temperature changes a catalyst's most pronounced effect. Potassium did not however appear to promote the carbon/CO₂ heterogeneous reaction which would have rejuvenated catalyst sites for further methane decomposition, as proposed in a previous study [1].

CO production behavior is similar to H₂ at these two temperatures. At low temperature, a potassium loading increase from 0.7 to 3.5 percent increases CO slightly. At high temperature, potassium loading decreases CO subtly between S and K0.7 feedstocks, but decreases CO significantly with a loading increase from 0.7 to 3.5 percent. At low temperature, CO was increased slightly as a result of increased secondary cracking reactions that were promoted by potassium. CO decreased because the dominant effect of potassium changes from decomposing methane witnessed at low temperatures, to inhibiting pyrolysis that is significant at high temperature.

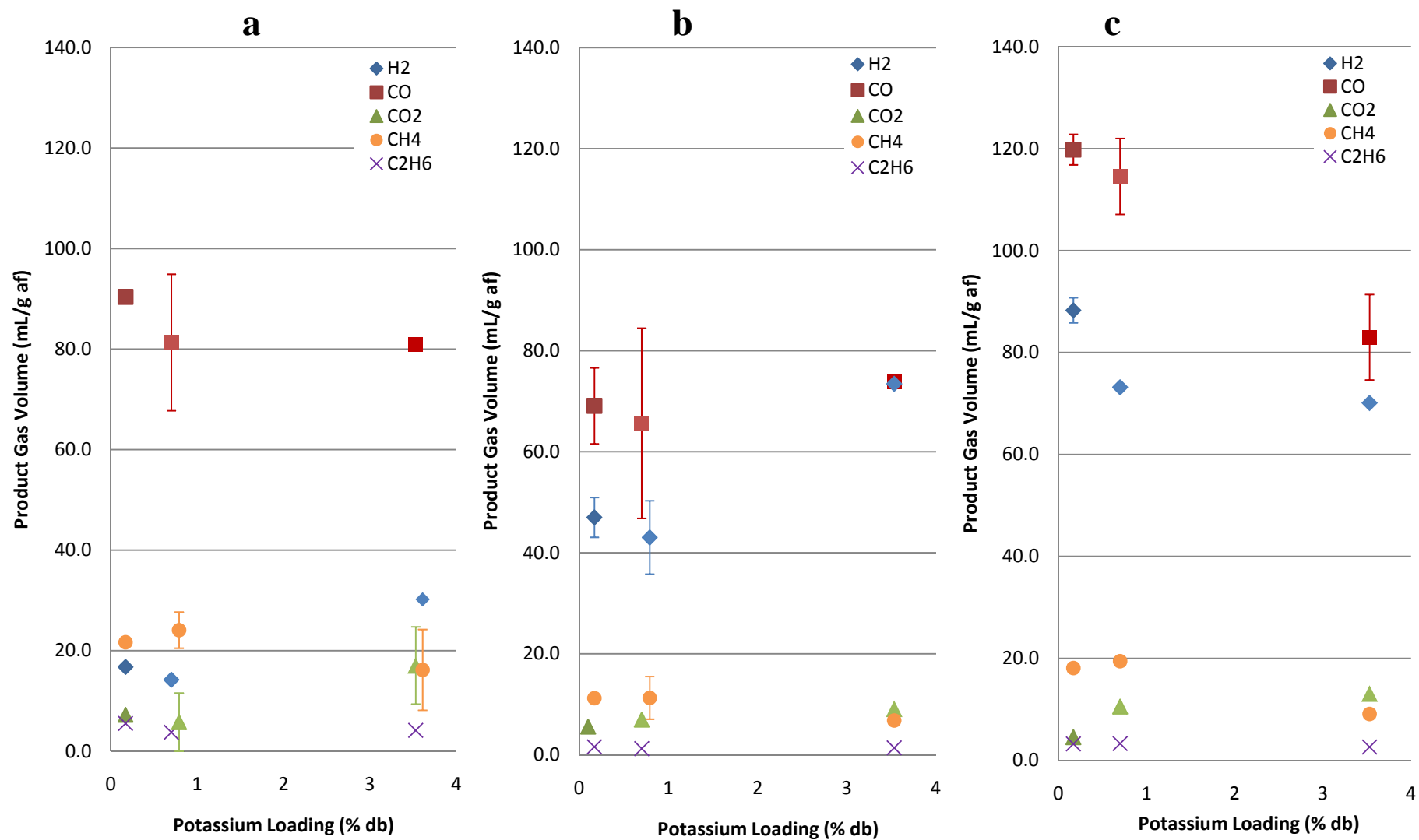


Figure 3.5: Product gas production versus potassium loading. a) CP at 700 °C; b) MWP at 700 °C; c) MWP at 1000 °C

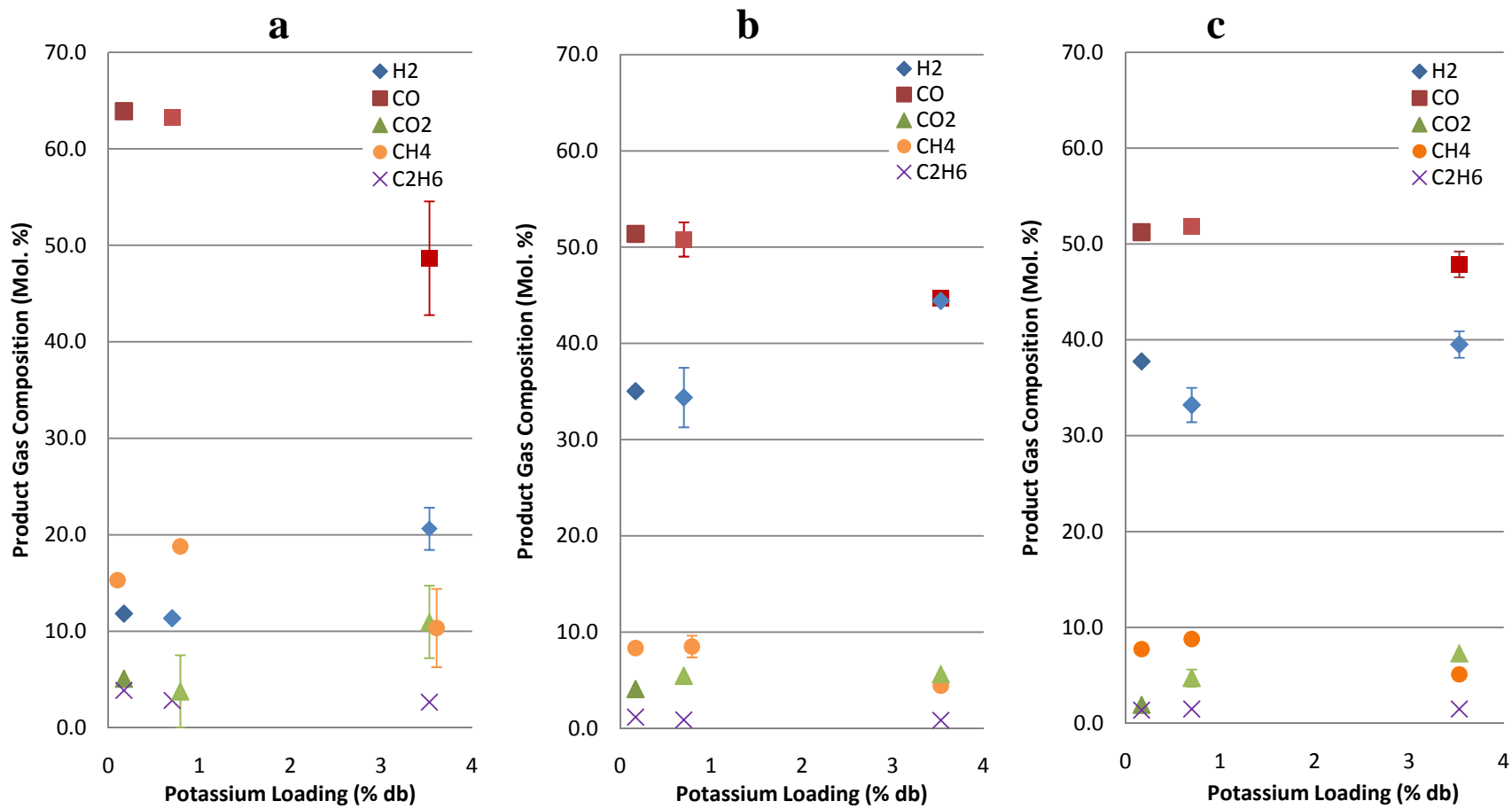


Figure 3.6: Product gas composition versus potassium loading. a) CP at 700 °C; b) MWP at 700 °C; c) MWP at 1000 °C

CO₂ increases for both pyrolysis temperatures; however, the higher temperature provided more CO₂ production. This means that the pyrolysis temperature increases the reactions of carboxylic functional groups to form CO₂.

3.3.3 Effect of Temperature

A summary of gas produced for each feedstock is plotted against temperature to compare the different feedstocks' response to temperature (see *Figure 3.4c*.) Temperature increases the syngas production of all feedstocks, however, the greater the potassium loading, the less significant this increase is. K3.5 syngas production remains roughly constant up to 900 °C, and increases gradually beyond this temperature. The increase in syngas due to temperature, as shown in *Figure 3.4a*, can be attributed to hydrogasification reactions. As discussed in the previous two sections, potassium's dominating effect on pyrolysis changes with temperature. That is why K3.5 is the best syngas producer at 700 °C and S is the best syngas producer at 1000 °C. Syngas production from S was greatest with temperature, jumping 101 ml/g (ash free) between pyrolysis temperatures of 700 and 1000°C. The total product gas and syngas volume relationships with temperature for K3.5 were found to be:

$$V_{\text{total gas}} = 9 \cdot 10^{-7} T^3 - 0.002 T^2 + 1.3014 T + 114.15$$

$$V_{\text{syngas}} = 7 \cdot 10^{-7} T^3 - 0.0013 T^2 + 0.5642 T + 116.74$$

For all feedstocks, production of all gas species showed an increase with a temperature increase from 700 to 1000 °C with the exceptions of CO₂ for S and H₂ for K3.5. This is because for temperatures between 700 and 900 °C, an increase in secondary cracking of heavy hydrocarbons at the expense of oil is evident in *Figure 3.7c*. Beyond 900 °C, the oil fraction remains relatively constant, and heterogeneous reactions are promoted at the expense of the char fraction (also evident in *Figure 3.7c*.) CO₂ is minutely reduced with increasing pyrolysis temperature in the case of S for an unknown reason, and in the case of K3.5, H₂ also remained fairly constant inexplicably.

In the case of K3.5, H₂ is shown to remain constant between pyrolysis temperatures of 700 and 1000 °C, but rises between 1000 °C and 1100 °C. This is because the hydrogasification reaction is promoted beyond 900 °C; however, the secondary cracking of oil fluctuated at 1000 °C,

offsetting the H₂ produced from hydrogasification. CO is shown to increase fairly linearly past 900 °C. This is also because of the promotion of hydrogasification beyond 900 °C. One possible explanation for this behavior is that cracking reactions rarely split C-O because of their relatively high bond energy.

CO₂ is shown to be maximized at 900 °C, which leads to the conclusion that carboxylic functional group reactions are maximized at this pyrolysis temperature.

3.4 Elemental Mass Balance

In order to make sure all elements from the initial corn stover feedstock were accounted for in the products, a mass balance was carried out on an ash free basis. Ultimate analysis was not carried out on the oil fractions of this experiment because oil was not produced in large enough quantities to meet the instruments' specifications. As a result, oil fractions were assumed to contain the same elemental makeup found in oil mallee derived oil discussed in the *Literature Review* section (see *Table 1.3*.) This bio-oil was selected because oil mallee's elemental makeup was the closest match to that of corn stover. Further study of *Table 1.3* shows that besides woody derived bio-oils, the elemental makeup is fairly consistent among the bio-oils discussed in this work.

The mass balance for each element contained in the initial feedstock is shown in *Table 3.6*. This table assumes that all moisture content was included into the elemental makeup of the initial feedstocks. Because of the way errors were calculated, positive errors mean that more of that element was found in the products than the initial feedstock contained, and negative errors mean that not all of said element contained in the initial feedstock was observed in the products. Each experiment's total mass were closed to less than 3.4 percent error, as shown in *Table 3.6*. Errors with regard to carbon, hydrogen and oxygen did not exceed 5.4, 2.6 and 4 percent, respectively. It can be observed that the greatest amount of error occurs in the electric furnace experiments. These larger errors are due to the procedural issue discussed in the *Gas Analysis* section, which led to significant sample drying before pyrolysis took place. Also, the error occurring in the microwave experiments is most likely due to water vapor that escaped the reactor unreacted, as an aqueous fraction was not observed in the condensing units, and *Table 3.6* includes all initial

moisture in calculations. The errors observed here are reasonable and prove that the analytic methods employed in this works were sufficiently accurate.

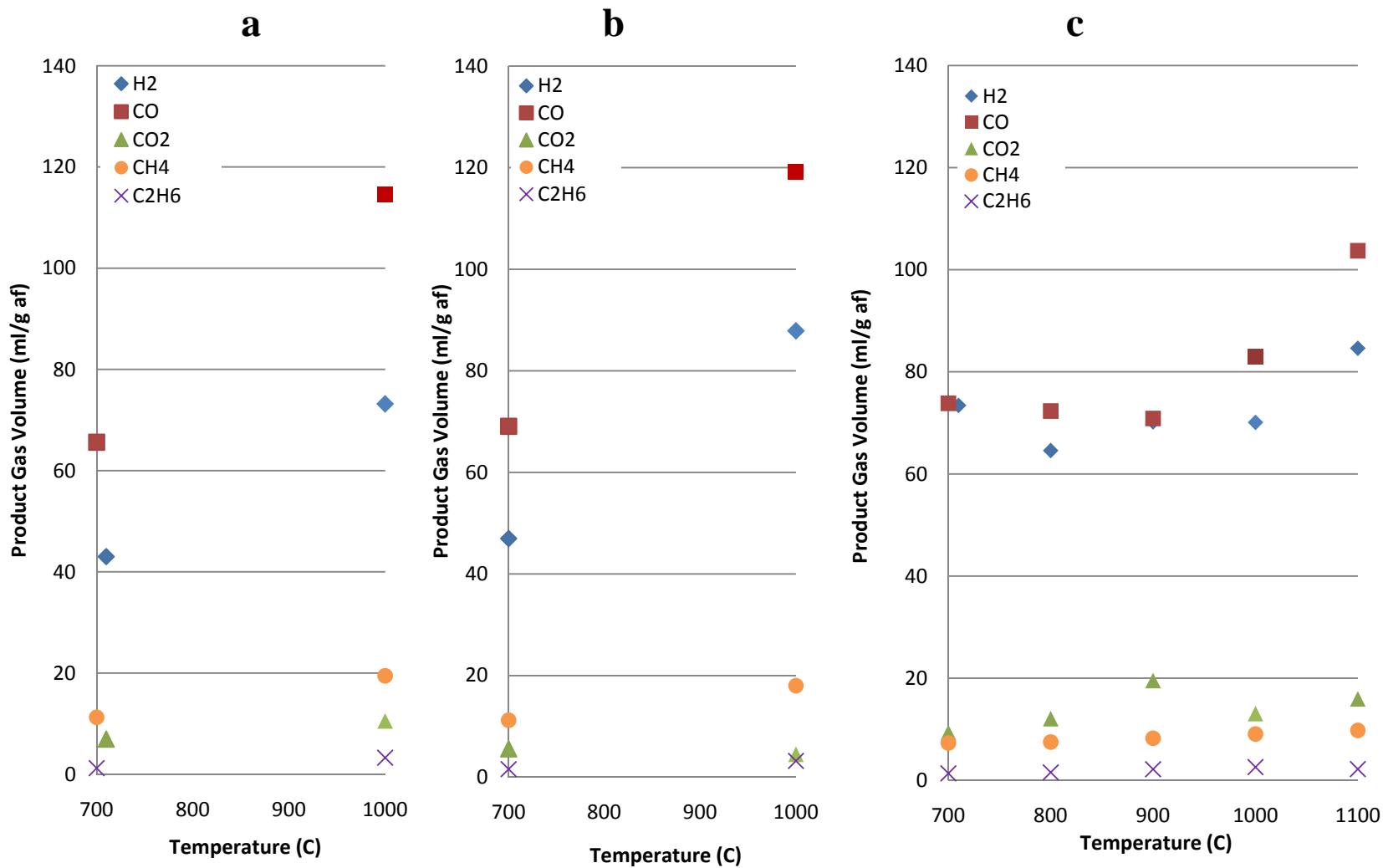


Figure 3.7: Product gas volume versus temperature for MWP. a) S; b) K0.7; c) K3.5

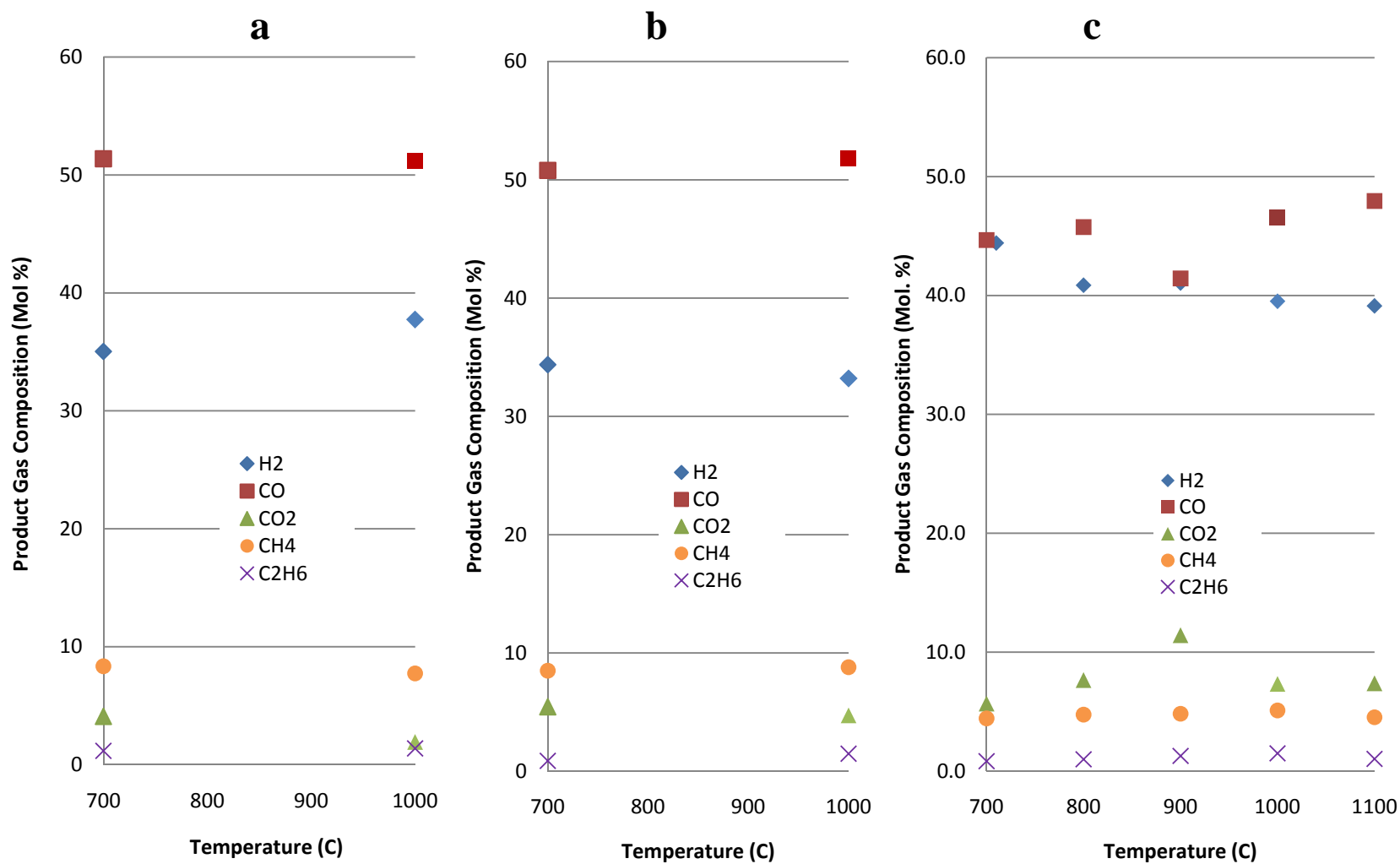


Figure 3.8: Product gas composition versus temperature for MWP. a) S; b) K0.7; c) K3.5

Table 3.6: Elemental Product Distribution. (Error: wt. % of element found in all products subtracted from the wt. % of element found in original feedstock)

CS	T (°C)	HM	Carbon				Hydrogen				Oxygen				Total
			Char	Bio-oil	Bio-gas	Error	Char	Bio-oil	Bio-gas	Error	Char	Bio-oil	Bio-gas	Error	Error
S	700	EF	22.9	1.9	75.2	5.4	-	4.2	95.8	-2.3	0.1	3.0	96.9	-3.8	-0.7
K0.7	700	EF	30.8	2.6	66.6	3.2	2.0	6.0	92.0	-2.1	-	4.8	95.2	-4.0	-2.9
K3.5	700	EF	30.8	2.5	66.7	2.8	2.3	6.1	91.7	-2.6	6.0	3.6	90.4	-3.6	-3.4
S	700	MW	20.5	10.0	69.6	1.8	-	15.3	84.7	-0.8	-	13.6	86.4	-0.3	0.8
K0.7	700	MW	26.8	14.5	58.7	0.0	-	23.3	76.7	-1.0	-	19.5	80.5	2.7	1.7
K3.5	700	MW	20.4	11.0	68.6	3.2	-	16.4	83.6	-0.4	2.1	14.8	83.0	-0.6	2.2
S	1000	MW	12.3	7.5	80.2	-0.1	-	9.8	90.2	-0.1	-	9.7	90.3	0.6	0.3
K0.7	1000	MW	18.2	10.0	71.9	-0.1	-	10.5	89.5	-0.7	-	3.5	96.5	2.0	1.2
K3.5	1000	MW	19.2	7.8	73.0	1.0	-	11.4	88.6	-0.6	-	9.7	90.3	1.1	1.6
K3.5	800	MW	22.8	8.6	68.7	1.6	-	12.9	87.1	-0.7	0.6	10.8	88.5	1.0	1.9
K3.5	900	MW	21.8	4.2	74.0	0.1	-	6.1	93.9	-0.7	-	5.0	95.0	2.2	1.6
K3.5	1100	MW	16.8	3.7	79.5	0.0	-	5.6	94.4	-0.9	-	4.4	95.6	2.7	1.8

Chapter 4

CONCLUSIONS AND RECOMMENDATIONS

4.1 Conclusions

This work discovered that potassium's main pyrolysis effects in order of descending influence are: inhibiting volatile release, promoting secondary cracking reactions of heavy hydrocarbons (oil) and promoting the decomposition reaction of methane at 700 °C. Potassium did not however appear to promote the carbon/CO₂ heterogeneous reaction which would have rejuvenated catalyst sites for further methane decomposition, as proposed in a previous study [1]. Potassium was shown to significantly inhibit the release of certain volatiles, such as oxygen containing compounds during pyrolysis at temperatures 700 to 1000 °C. The result from this is a much larger char fraction when potassium was added. This inhibiting effect of potassium was found to be prominent at higher temperatures in MWP.

A consistent trend among all temperatures tested in this study was that in MWP, potassium addition decreased the oil fraction produced. This means that potassium promoted the secondary reactions that broke down the heavy hydrocarbons into incondensable gases.

A potassium loading between 0.7 and 3.5 percent was found to promote the decomposition of methane reaction at 700 °C, but not at 1000 °C. The reason why the decomposition of methane was not observed at the higher temperature is because at higher temperatures, potassium's pyrolysis inhibiting affect is the dominant effect. As a result of this, there was no evident significant increase in H₂ at the expense of CH₄. Potassium's promotion of the decomposition of methane was 60 percent more pronounced in MWP compared to CP at 700 °C. A possible reason for this difference is that in microwave heating, the potassium could have achieved temperatures much higher than the rest of the sample, thus further promoting methane's decomposition. A potassium loading between 0.7 and 3.5 percent promotes the decomposition of methane reaction.

The experiment that showed the best syngas production was the S (stripped) feedstock brought to 1000 °C in the microwave. This experiment yielded 88 ml/g (ash free) of H₂ and 120 ml/g (ash free) of CO.

4.2 Recommendations for Future Work

Calibrating a sample's emissivity is currently guess work, as there are very few resources on this topic; however an accurate measurement of an object's emissivity is imperative to accurately monitor high sample temperatures inside of a microwave. A standard procedure needs to be established for calibrating a sample's emissivity at various temperatures.

Microwave pyrolysis of biomass has not yet been demonstrated on even a pilot scale in order to show that the energy content of the fuel coming out of the process is greater than the electricity input into the microwave processing. A continuous feed study would also be of great value to discover any problematic issues that arise in a more realistic microwave pyrolysis setup. If this process does not turn out to be energy positive, the electricity going into the microwave would be better off powering the community. This aspect of microwave pyrolysis needs to be addressed to decide if microwave heating is indeed a more energy efficient process than conventional biomass gasification (considered the future in conventional conversion methods for power production.)

Moisture inherent to biomass is important in syngas production through microwave pyrolysis. A study detailing the effects of syngas production due to slight changes of moisture in the biomass sample would help determine the balance between syngas production, and microwave processing's energy requirement.

References

1. Dominguez, A., et al., *Bio-syngas production with low concentrations of CO₂ and CH₄ from microwave-induced pyrolysis of wet and dried sewage sludge*. Chemosphere, 2008. **70**(3): p. 397-403.
2. Peelamedu, R., R. Roy, and D. Agrawal, *Anisothermal reaction synthesis of garnets, ferrites, and spinels in microwave field*. Materials research bulletin, 2001. **36**(15): p. 2723-2739.
3. Perlack, R., Wright, L., Turhollow, A., Graham, R., *Biomass as Feedstock for a Bioenergy and Bioproducts Industry: The Technical Feasibility of a Billion-Ton Annual Supply*. 2005, Oak Ridge National Laboratory.
4. Rezaiyan, J., N. C., *Gasification Technologies: A Primer for Engineers and Scientists*. 2005, Boca Raton, FL: Taylor & Francis.
5. Dominguez, A., et al., *Conventional and microwave induced pyrolysis of coffee hulls for the production of a hydrogen rich fuel gas*. Journal of Analytical and Applied Pyrolysis, 2007. **79**(1-2): p. 128-135.
6. Menendez, J.A., et al., *Evidence of self-gasification during the microwave-induced pyrolysis of coffee hulls*. Energy & Fuels, 2007. **21**(1): p. 373-378.
7. Domínguez, A., et al., *Microwave-assisted catalytic decomposition of methane over activated carbon for CO₂-free hydrogen production*. International Journal of Hydrogen Energy, 2007. **32**(18): p. 4792-4799.
8. Dominguez, A., et al., *Gas chromatographic-mass spectrometric study of the oil fractions produced by microwave-assisted pyrolysis of different sewage sludges*. Journal of Chromatography A, 2003. **1012**(2): p. 193-206.
9. Dominguez, A., et al., *Production of bio-fuels by high temperature pyrolysis of sewage sludge using conventional and microwave heating*. Bioresource Technology, 2006. **97**(10): p. 1185-1193.
10. Park, E.S., B.S. Kang, and J.S. Kim, *Recovery of oils with high caloric value and low contaminant content by pyrolysis of digested and dried sewage sludge containing polymer flocculants*. Energy & Fuels, 2008. **22**(2): p. 1335-1340.
11. Sanchez, M.E., et al., *Pyrolysis of mixtures of sewage sludge and manure: A comparison of the results obtained in the laboratory (semi-pilot) and in a pilot plant*. Waste Management, 2007. **27**(10): p. 1328-1334.
12. Miao, X.L., Q.Y. Wu, and Wd, *High yield bio-oil production from fast pyrolysis by metabolic controlling of *Chlorella protothecoides**. Journal of Biotechnology, 2004. **110**(1): p. 85-93.
13. Miao, X.L., et al., *Fast pyrolysis of microalgae to produce renewable fuels*. Journal of Analytical and Applied Pyrolysis, 2004. **71**(2): p. 855-863.

14. Garcia-Perez, M., et al., *Fast pyrolysis of oil mallee woody biomass: Effect of temperature on the yield and quality of pyrolysis products*. Industrial & Engineering Chemistry Research, 2008. **47**(6): p. 1846-1854.
15. Raveendran, K., *Influence of mineral matter on biomass pyrolysis characteristics*. Fuel, 1995. **74**(12): p. 1812.
16. Ringer, M., V. Putsche, J. Scahill, *Large-Scale Pyrolysis Oil Production: A Technology Assessment and Economic Analysis*. 2006, National Renewable Energy Laboratory.
17. Miura, M., et al., *Rapid pyrolysis of wood block by microwave heating*. Journal of Analytical and Applied Pyrolysis, 2004. **71**(1): p. 187-199.
18. Sondreal, E.A., and G. Wiltsee, *LOW-RANK COAL: Its Present and Future-Role in the United States*. 1984.
19. Parikh, J., S.A. Channiwala, and G.K. Ghosal, *A correlation for calculating HHV from proximate analysis of solid fuels*. Fuel, 2005. **84**(5): p. 487-494.
20. Raveendran, K., A. Ganesh, and K.C. Khilar, *Influence of mineral matter on biomass pyrolysis characteristics*. Fuel, 1995. **74**(12): p. 1812-1822.
21. Otto, K., L. Bartosiewicz, and M. Shelef, *Effects of calcium, strontium, and barium as catalysts and sulphur scavengers in the steam gasification of coal chars*. Fuel, 1979. **58**(8): p. 565-572.
22. Moulijn, J.A., F. Kapteign, ed. *Carbon and Coal Gasification*. 1986, Martinus Nijhoff Publishers. 181-195.
23. Demirbas, A., *Hydrogen production from biomass by the gasification process*. Energy sources, 2002. **24**(1): p. 59-68.
24. Dominguez, A., et al., *Biogas to syngas by microwave-assisted dry reforming in the presence of char*. Energy & Fuels, 2007. **21**(4): p. 2066-2071.
25. Bradbury, A., Y. Sakai, and F. Shafizadeh, *KINETIC-MODEL FOR PYROLYSIS OF CELLULOSE*. Journal of Applied Polymer Science, 1979. **23**(11): p. 3271-3280.
26. Kuchonthara, P., T. Vitidsant, and A. Tsutsumi, *Catalytic effects of potassium on lignin steam gasification with γ -Al₂O₃ as a bed material*. Korean Journal of Chemical Engineering, 2008. **25**(4): p. 656-662.
27. Tomita, A., T. Takarada, and Y. Tamai, *Gasification of coal impregnated with catalyst during pulverization: effect of catalyst type and reactant gas on the gasification of Shin-Yubari coal*. Fuel, 1983. **62**(1): p. 62-68.
28. Nowakowski, D.J., et al., *Potassium catalysis in the pyrolysis behaviour of short rotation willow coppice*. Fuel, 2007. **86**(15): p. 2389-2402.
29. Nowakowski, D.J. and J.M. Jones, *Uncatalysed and potassium-catalysed pyrolysis of the cell-wall constituents of biomass and their model compounds*. Journal of Analytical and Applied Pyrolysis, 2008. **83**(1): p. 12-25.

30. Nowakowski, D., et al., *Survey of influence of biomass mineral matter in thermochemical conversion of short rotation willow coppice*. Journal of the Institute of Energy, 2008. **81**(4): p. 234-241.
31. Dominguez, A., J.A. Menendez, and J.J. Pis, *Hydrogen rich fuel gas production from the pyrolysis of wet sewage sludge at high temperature*. Journal of Analytical and Applied Pyrolysis, 2006. **77**(2): p. 127-132.
32. Wang, X., et al., *The Influence of Microwave Drying on Biomass Pyrolysis*. Energy Fuels, 2008. **22**(1): p. 67-74.
33. Hwang, I.H., Y. Ouchi, and T. Matsuto, *Characteristics of leachate from pyrolysis residue of sewage sludge*. Chemosphere, 2007. **68**(10): p. 1913-1919.
34. Shen, L. and D.K. Zhang, *An experimental study of oil recovery from sewage sludge by low-temperature pyrolysis in a fluidized-bed*. Fuel, 2003. **82**(4): p. 465-472.
35. Dominguez, A., et al., *Investigations into the characteristics of oils produced from microwave pyrolysis of sewage sludge*. Fuel Processing Technology, 2005. **86**(9): p. 1007-1020.
36. Menendez, J.A., et al., *Microwave-induced drying, pyrolysis and gasification (MWDPG) of sewage sludge: Vitrification of the solid residue*. Journal of Analytical and Applied Pyrolysis, 2005. **74**(1-2): p. 406-412.
37. Menendez, J.A., et al., *Microwave pyrolysis of sewage sludge: analysis of the gas fraction*. Journal of Analytical and Applied Pyrolysis, 2004. **71**(2): p. 657-667.
38. Menendez, J.A., et al., *Microwave-induced pyrolysis of sewage sludge*. Water Research, 2002. **36**(13): p. 3261-3264.
39. Stein, D., Edgar, R., Iskander, M., *Microwave Processing Of Materials*. 1994, National Academy of Sciences: Washington, D.C. p. 5-38.
40. Jones, D.A., et al., *Microwave heating applications in environmental engineering - a review*. Resources Conservation and Recycling, 2002. **34**(2): p. 75-90.
41. Savova, D., et al., *Biomass conversion to carbon adsorbents and gas*. Biomass & Bioenergy, 2001. **21**(2): p. 133-142.
42. Ischia, M., et al., *Pyrolysis study of sewage sludge by TG-MS and TG-GC-MS coupled analyses*. Journal of Thermal Analysis and Calorimetry, 2007. **87**(2): p. 567-574.
43. Storm, C., et al., *Co-pyrolysis of coal/biomass and coal/sewage sludge mixtures*. Journal of Engineering for Gas Turbines and Power-Transactions of the Asme, 1999. **121**(1): p. 55-63.
44. Iwasaki, W., *A consideration of the economic efficiency of hydrogen production from biomass*. International Journal of Hydrogen Energy, 2003. **28**(9): p. 939-944.
45. Conesa, J.A., et al., *Evolution of gases in the primary pyrolysis of different sewage sludges*. Thermochemica Acta, 1998. **313**(1): p. 63-73.

46. Acikgoz, C., O. Onay, and O.M. Kockar, *Fast pyrolysis of linseed: product yields and compositions*. Journal of Analytical and Applied Pyrolysis, 2004. **71**(2): p. 417-429.
47. Yu, F., R. Ruan, et al., *Microwave Pyrolysis of Biomass*. 2006: St. Joseph, MI: ASABE.
48. El harfi, K., et al., *Pyrolysis of the Moroccan (Tarfaya) oil shales under microwave irradiation*. Fuel, 2000. **79**(7): p. 733-742.
49. Fidalgo, B., et al., *Microwave-assisted dry reforming of methane*. International Journal of Hydrogen Energy, 2008. **33**(16): p. 4337-4344.
50. Fidalgo, B., et al., *Microwave-assisted pyrolysis of CH₄/N₂ mixtures over activated carbon*. Journal of Analytical and Applied Pyrolysis, 2008. **82**(1): p. 158-162.
51. Gélinas, Y., J.A. Baldock, and J.I. Hedges, *Demineralization of marine and freshwater sediments for CP/MAS ¹³C NMR analysis*. Organic Geochemistry, 2001. **32**(5): p. 677-693.
52. Inguanzo, M., et al., *On the pyrolysis of sewage sludge: the influence of pyrolysis conditions on solid, liquid and gas fractions*. Journal of Analytical and Applied Pyrolysis, 2002. **63**(1): p. 209-222.
53. Morgan, B. and A. Scaroni, *THE EFFECTS OF CATIONS ON PULVERIZED COAL COMBUSTION*. Abstracts of papers, 1983. **186**(AUG): p. 71-FUEL.
54. Nik-Azar, M., et al., *Mineral matter effects in rapid pyrolysis of beech wood*. Fuel Processing Technology, 1997. **51**(1-2): p. 7-17.
55. Madorsky, S., V. Hart, and S. Straus, *PYROLYSIS OF CELLULOSE IN A VACUUM*. Journal of research of the National Bureau of Standards, 1956. **56**(6): p. 343-354.
56. Essig, M., Richards, G. N., Schenck, E, *Cellulose and Wood - Chemistry and Technology*, ed. Schuerch. 1989, New York: Wiley.
57. Vamvuka, D., S. Troulinos, and E. Kastanaki, *The effect of mineral matter on the physical and chemical activation of low rank coal and biomass materials*. Fuel, 2006. **85**(12-13): p. 1763-1771.
58. Wei, X., et al., *Transformation of Alkali Metals during Pyrolysis and Gasification of a Lignite*. Energy & Fuels, 2008. **22**(3): p. 1840-1844.
59. Zhang, J., et al., *The varying characterization of alkali metals (Na, K) from coal during the initial stage of coal combustion*. Energy & Fuels, 2001. **15**(4): p. 786-793.
60. Zhang, J., Han, C., Liu, K., Xu, Y., *Various forms of alkali metal in coal and its behaviour during combustion*. Journal of Engineering for Thermal Energy and Power, 1999. **14**(2): p. 83-85.
61. Wei, X.F., et al., *Transformation of alkali metals during pyrolysis and gasification of a lignite*. Energy & Fuels, 2008. **22**(3): p. 1840-1844.
62. Lee, K.H., *Influence of reaction temperature, pretreatment, and a char removal system on the production of bio-oil from rice straw by fast pyrolysis, using a fluidized bed*. Energy & Fuels, 2005. **19**(5): p. 2179.